Copy
RM L55A21

329

NACA

RESEARCH MEMORANDUM

STATIC LONGITUDINAL AND LATERAL STABILITY DATA FROM AN

EXPLORATORY INVESTIGATION AT MACH NUMBER 4.06 OF AN

AIRPLANE CONFIGURATION HAVING A WING

OF TRAPEZOIDAL PLAN FORM

By Robert W. Dunning and Edward F. Ulmann

Langley Aeronautical Laboratory
Langley Field, Va.

NATIONAL ADVISORY COMMITTEE
FOR AERONAUTICS

WASHINGTON

February 15, 1955

CONFIDENTIAL

NATIONAL ADVISORY COMMITTEE FOR AERONAUTICS

———

RESEARCH MEMORANDUM

———

STATIC LONGITUDINAL AND LATERAL STABILITY DATA FROM AN

EXPLORATORY INVESTIGATION AT MACH NUMBER 4.06 OF AN

AIRPLANE CONFIGURATION HAVING A WING

OF TRAPEZOIDAL PLAN FORM

By Robert W. Dunning and Edward F. Ulmann

SUMMARY

An investigation to determine the static longitudinal and lateral stability characteristics of an airplane configuration having a trapezoidal wing with modified hexagonal airfoil section and a cruciform tail with 5° semiangle wedge section has been carried out in the Langley 9- by 9-inch Mach number 4 blowdown jet. Tests on the complete airplane and various combinations of its components were made at a Mach number of 4.06 and a Reynolds number of 2.7×10^6, based on wing mean aerodynamic chord. Data were obtained for angles of attack from 0° to a maximum of 8° to 20°, at angles of sideslip from 0° up to a maximum of 5° to 8°, the maximum values depending on the configuration tested. The data are presented with respect to body axes except for lift and drag which are referred to the stability axes.

INTRODUCTION

The aircraft configurations previously investigated experimentally at high supersonic and hypersonic speeds have been restricted to missiles which were not required to land, and which therefore had relatively small wings or wings of very low aspect ratio. The purpose of the present investigation was to determine the characteristics of a configuration conforming more closely to a piloted aircraft having a wing area sufficient for conventional landing. Of the various possible configurations, one was selected for this exploratory study which was expected to have satisfactory low-speed characteristics and satisfactory transonic characteristics. This configuration (fig. 1) employs a trapezoidal wing and the arrangement, in general, is similar to that of conventional airplanes.

Two particular features were incorporated which are believed to be desirable for high supersonic and hypersonic operation - relatively large leading-edge radii for both wing and tail and wedge-shaped sections for the tail surfaces. The wing and tail sections were designed with large leading-edge radii because of heat-transfer considerations at high Mach numbers. The wing leading-edge radius, for example, would be approximately 1.5 inches at the wing-fuselage intersection for a full-size airplane having a wing span of about 28 feet. Inasmuch as the effectiveness of lifting surfaces having flat-plate or conventional airfoil sections decreases considerably with Mach number at high supersonic speeds (ref. 1), the effectiveness of tail surfaces of conventional size utilizing these airfoil sections would be marginal or insufficient at the Mach number of the present tests. Several types of tail airfoil sections therefore are being considered and the present results were obtained with a 5° semiangle wedge section.

In references 2 and 3, longitudinal and lateral stability data were presented for this same configuration at Mach number 6.86. This report presents the static longitudinal and lateral stability characteristics at Mach number 4.06 without analysis in order to expedite publication.

SYMBOLS

The results of the tests are presented as standard NACA coefficients of forces and moments. The data are referred to the body axes except for lift and drag which are referred to the stability axes (fig. 2), with the reference center of gravity at 52.66 percent body length from the body nose (54 percent mean aerodynamic chord).

C_N normal-force coefficient, $-Z_B/qS$

C_L lift coefficient, $-Z_S/qS$

C_{D_T} total drag coefficient, $-X_{B_T}/qS$

C_{D_B} base drag coefficient, $-X_{B_B}/qS$

$C_{m_{c.g.}}$ pitching-moment coefficient about center of gravity, $M'/qS\bar{c}$

C_Y lateral-force coefficient, Y/qS

C_n yawing-moment coefficient about center of gravity, N/qSb

C_l rolling-moment coefficient, L/qSb

Z_B force along Z_B-axis

Z_S force along Z_S-axis

X_{B_T} total force along X_B-axis

X_{B_B} force along X_B-axis contributed by base

M' moment about Y-axis

Y force along Y-axis

N moment about Z_B-axis

L moment about X_B-axis

q free-stream dynamic pressure

S total wing area, including body intercept

$\bar{c}$ wing mean aerodynamic chord

b wing span

L/D_T lift-drag ratio, C_L/C_{D_T}

R Reynolds number based on $\bar{c}$

M Mach number

c.p.   longitudinal distance from nose to center of pressure, percent body length

α angle of attack of fuselage center line, deg

β angle of sideslip, deg

$\dfrac{\partial C_m}{\partial C_L}$ rate of change of pitching-moment coefficient with lift coefficient

C_{n_β} rate of change of yawing-moment coefficient with angle of sideslip

C_{l_β} rate of change of rolling-moment coefficient with angle of
sideslip

C_{Y_β} rate of change of lateral-force coefficient with angle of
sideslip

APPARATUS

The tests were conducted in the Langley 9- by 9-inch Mach number 4
blowdown jet, which is described and for which a calibration is given
in reference 4. The settling-chamber pressure, which was held constant
by a pressure-regulating valve, and the corresponding air temperature
were continuously recorded during each run.

Two separate internal strain-gage balances were used to obtain the
data. One balance measured normal force, pitching moment, side force,
yawing moment, and rolling moment. The second balance measured chord
force through the angle-of-attack range but was limited to measurements
at zero angle of sideslip because of balance design.

Representative schlieren photographs of the flow around the model
were made by the use of an off-axis, single-pass, two-mirror schlieren
system. Exposure time was 1/200 second, and the knife edge was oriented
parallel to the free-stream flow.

MODELS

The model configurations used for the present tests consisted of a
complete airplane (fig. 1), a body alone, a body-wing combination, and
a body-tail combination. Details concerning the airplane model are given
in the three-view drawing (fig. 3(a)), in the sketches of the airfoil
sections (fig. 3(b)), and in the table of geometric characteristics
(table I). The wing and tail sections were designed with large leading-
edge radii because of heat-transfer considerations at high Mach numbers.
A photograph of the complete airplane configuration installed in the
Langley 9- by 9-inch Mach number 4 blowdown jet is presented in figure 4.

TESTS

The settling-chamber stagnation temperature during any single run
varied from approximately 80° to 40° F, and the settling-chamber stag-
nation pressure was held at approximately 186 lb/sq in. abs. These con-
ditions correspond approximately to a Reynolds number of 2.7×10^6, based

on the wing mean aerodynamic chord. The tests were run at humidities below 5×10^{-6} pounds of water vapor per pound of dry air, which is believed to be low enough to eliminate water-condensation effects. The test-section static temperature and pressure did not reach the point where liquefaction of air would take place. Data were obtained for angles of attack from 0° to a maximum of 8° to 20°, at angles of sideslip from 0° to a maximum of 5° to 8°, the maximum values depending on the configuration tested. Base drag data were obtained from static pressures measured at the base of the model.

PRECISION OF DATA

The probable uncertainties in the test data due to the accuracy limitations of the balances and the recording equipment and the ability of the system to repeat data points are listed in the table below. The low accuracy of the rolling-moment coefficients relative to the maximum rolling-moment encountered should be noted. This occurred because rolling-moment gages were added to an existing balance which was not originally designed to measure rolling moment.

C_N . . . . ± 0.001

C_L . . . . ± 0.001

C_{D_T} . . . . ± 0.0003

$C_{m_{c.g.}}$ . . . . ± 0.0004

C_Y . . . . ± 0.0003

C_n . . . . ± 0.00005

C_l . . . . ± 0.0009

α, deg . . . . ± 0.1

β, deg . . . . ± 0.1

RESULTS

The experimental static aerodynamic characteristics of the models are given for all angles of attack and sideslip in tables II and III, and representative portions of the data are presented in the figures. Equations for transferring these coefficients from the body axes to the stability axes are presented in the appendix. The variations with angle of attack of the longitudinal characteristics of the complete airplane and various combinations of its components are presented in figures 5

to 11. In figures 12 and 13 some static longitudinal stability charac-
teristics are presented.

The variations with sideslip angle of the lateral characteristics
of the body-wing and complete-airplane configurations are presented in
figure 14, and the variations with sideslip angle of the longitudinal
characteristics of the body-wing and complete-airplane configurations
are presented in figure 15. The effects of normal-force coefficient on
the lateral characteristics for the body-wing and complete configurations
are presented in figure 16. Some static lateral stability character-
istics are presented in figure 17.

Typical schlieren photographs of the components at a constant angle
of attack and of the complete model at various angles of attack are pre-
sented in figures 18 and 19. The closely spaced disturbances which can
be seen extending downstream at the top and the bottom of the schlieren
field of view are caused by the tips of 1/4-inch-diameter rods which
support the model against shock loads during the starting and stopping
cycles of the tunnel. The rods are withdrawn into or almost into the
tunnel floor and ceiling while data are being taken. The plugged holes
in the tunnel floor used for these rods may be seen in figure 4. It
should be noted that the model pivots in pitch about a point near the
base of the body, and that consequently the tail fins do not move up or
down into that part of the flow influenced by the disturbances from the
support rods.

Langley Aeronautical Laboratory,
    National Advisory Committee for Aeronautics,
        Langley Field, Va., January 3, 1955.

APPENDIX

The equations for transfer of force and moment coefficients from the body-axis system to the stability-axis system (fig. 2) are as follows:

$$C_{Y_S} = C_{Y_B}$$

$$C_{l_S} = C_{l_B} \cos \alpha + C_{n_B} \sin \alpha$$

$$C_{n_S} = C_{n_B} \cos \alpha - C_{l_B} \sin \alpha$$

$$C_{m_S} = C_{m_B}$$

Since longitudinal forces were measured only for $\beta = 0$, the axis-transfer equations for C_{L_S} and C_{D_S} are not given here.

REFERENCES

1. McLellan, Charles H.: A Method for Increasing the Effectiveness of
     Stabilizing Surfaces at High Supersonic Mach Numbers. NACA
     RM L54F21, 1954.

2. Penland, Jim A., Ridyard, Herbert W., and Fetterman, David E., Jr.:
     Lift, Drag, and Static Longitudinal Stability Data From an Explor-
     atory Investigation at a Mach Number of 6.86 of an Airplane Con-
     figuration Having a Wing of Trapezoidal Plan Form. NACA RM L54L03b,
     1955.

3. Ridyard, Herbert W., Fetterman, David E., Jr., and Penland, Jim A.:
     Static Lateral Stability Data From an Exploratory Investigation at
     a Mach Number of 6.86 of an Airplane Configuration Having a Wing
     of Trapezoidal Plan Form. NACA RM L55A21a, 1955.

4. Ulmann, Edward F., and Lord, Douglas R.: An Investigation of Flow
     Characteristics at Mach Number 4.04 Over 6- and 9-Percent-Thick
     Symmetrical Circular-Arc Airfoils Having 30-Percent-Chord Trailing-
     Edge Flaps. NACA RM L51D30, 1951.

TABLE I.- GEOMETRIC CHARACTERISTICS OF MODEL

Wing:
    Area (including area submerged in fuselage), sq in. 6.24
    Span, in. 4.33
    Mean aerodynamic chord, in. 1.716
    Root chord, in. 2.53
    Tip chord, in. 0.354
    Airfoil section . . . .   hexagonal with round leading edge
    Taper ratio 0.140
    Aspect ratio 3.00
    Sweep of leading edge, deg 38.83
    Sweep of quarter-chord line, deg   29
    Incidence at fuselage center line, deg   0
    Dihedral, deg   0
    Geometric twist; deg   0

Horizontal tail or vertical tail:
    Area (including area submerged in fuselage), sq in. 2.06
    Span, in. 2.69
    Mean aerodynamic chord, in. 0.853
    Root chord, in. 1.214
    Tip chord, in. 0.317
    Airfoil section . . . .   5° semiangle wedge
    Taper ratio 0.261
    Aspect ratio 3.52
    Sweep of leading edge, deg 22.63
    Dihedral, deg   0

Fuselage:
    Length, in. 7.50
    Maximum diameter, in. 0.790
    Fineness ratio 9.50
    Base diameter, in. 0.790
    Distance from nose to moment reference 3.950
    Ogive nose length, in. 2.29
    Ogive radius, in. 6.85

TABLE II.- STATIC LONGITUDINAL AND LATERAL AERODYNAMIC CHARACTERISTICS

OF AN AIRPLANE CONFIGURATION AND VARIOUS COMBINATIONS OF ITS

COMPONENTS. BODY AXIS DATA. M = 4.06. R = 2.7 × 10^6.

(a) Body-wing-tail

α	β	C_N	$C_{m_{c.g.}}$	c.p.	C_Y	C_n	C_l
0.0	0.0	−0.0023	0.0001	53.7	−0.0001	0.0001	0.0009
↓	1.0	−.0023	.0002	54.7	−.0110	.0026	.0008
	2.0	−.0017	0.0	52.7	−.0223	.0050	.0007
	3.0	−.0017	0.0	52.7	−.0341	.0077	.0004
	4.0	−.0016	0.0	52.7	−.0454	.0102	.0003
↓	5.0	−.0048	.0011	57.9	−.0570	.0124	.0004
2.0	0.0	0.0484	−0.0125	58.6	0.0010	0.0	.0002
↓	1.0	.0484	−.0127	58.7	−.0102	.0025	.0001
	2.0	.0483	−.0129	58.8	−.0215	.0050	0.0
	3.0	.0472	−.0129	58.9	−.0334	.0076	0.0
	4.0	.0466	−.0131	59.1	−.0451	.0101	.0006
↓	5.0	.0461	−.0131	59.2	−.0571	.0124	.0006
4.0	0.0	0.1002	−0.0248	58.3	0.0020	−0.0002	0.0
↓	0.0	.1009	−.0253	58.4	.0019	−.0002	.0011
	0.0	.1019	−.0256	58.4	.0024	−.0002	−.0004
	1.0	.1025	−.0255	58.4	−.0098	.0023	.0014
	1.0	.1020	−.0256	58.4	−.0095	.0023	−.0003
	2.0	.1025	−.0257	58.4	−.0208	.0048	.0015
	2.0	.1016	−.0257	58.5	−.0206	.0047	−.0002
	3.0	.1032	−.0256	58.4	−.0329	.0074	.0011
	3.0	.1019	−.0258	58.5	−.0330	.0074	0.0
	4.0	.1037	−.0256	58.3	−.0458	.0101	.0009
	4.0	.1019	−.0259	58.5	−.0455	.0100	.0002
	5.0	.1038	−.0258	58.4	−.0579	.0125	.0009
↓	5.0	.1024	−.0262	58.5	−.0575	.0125	0.0
6.0	0.0	0.1614	−0.0408	58.5	0.0029	−0.0003	0.0001
↓	1.0	.1554	−.0387	58.4	−.0091	.0024	.0001
	2.0	.1546	−.0380	58.3	−.0204	.0047	.0004
	3.0	.1557	−.0378	58.2	−.0335	.0074	.0004
↓	4.0	.1554	−.0374	58.2	−.0450	.0099	.0006

TABLE II.- STATIC LONGITUDINAL AND LATERAL AERODYNAMIC CHARACTERISTICS OF AN

AIRPLANE CONFIGURATION AND VARIOUS COMBINATIONS OF ITS COMPONENTS.

BODY AXIS DATA. $M = 4.06$. $R = 2.7 \times 10^6$ - Continued

(a) Body-wing-tail - Concluded

α	β	C_N	$C_{m_{c.g.}}$	c.p.	C_Y	C_n	C_l
8.0	0.0	0.2142	-0.0534	58.4	0.0033	-0.0003	-0.0004
↓	1.0	.2142	-.0531	58.3	-.0098	.0025	-.0002

(b) Body

0.0	0.0	-0.0017	-0.0011	37.9	-0.0002	0.0001	0.0005
2.0	0.0	.0067	.0085	23.6	.0001	.0002	.0009
4.0	0.0	.0178	.0184	29.0	.0003	.0003	.0009
6.0	0.0	.0327	.0248	35.3	.0005	.0002	.0008
8.0	0.0	.0502	.0271	40.3	.0011	.0002	.0007
10.0	0.0	.0709	.0301	43.0	.0011	.0002	.0004
12.0	0.0	.0908	.0338	44.2	.0017	.0003	.0001
14.0	0.0	.1119	.0378	44.9	.0022	.0004	-.0004
15.0	0.0	.1220	.0390	45.4	.0019	.0003	.0009
16.0	0.0	.1326	.0398	45.8	.0021	.0004	.0008
18.0	0.0	.1585	.0401	46.9	.0026	.0004	.0003
20.0	0.0	.1858	.0402	47.7	.0043	.0003	.0002

(c) Body-wing

0.0	0.0	0.0045	0.0009	48.1	0.0007	0.0001	0.0015
	1.0	.0050	.0009	48.6	-.0034	-.0016	.0013
	2.0	.0029	.0007	47.2	-.0083	-.0034	.0013
	3.0	.0025	.0005	48.1	-.0129	-.0051	.0010
	4.0	.0004	0.0	52.7	-.0182	-.0067	.0006
	5.0	-.0011	-.0003	46.4	-.0236	-.0080	.0003
	6.0	-.0021	-.0004	48.3	-.0307	-.0091	-.0001
	7.0	-.0006	-.0001	48.9	-.0387	-.0098	.0004
↓	8.0	-.0001	0.0	52.7	-.0477	-.0103	.0007

TABLE II.- STATIC LONGITUDINAL AND LATERAL AERODYNAMIC CHARACTERISTICS

OF AN AIRPLANE CONFIGURATION AND VARIOUS COMBINATIONS OF ITS

COMPONENTS. BODY AXIS DATA. M = 4.06.

R = 2.7 × 10^6 - Continued

(c) Body-wing - Continued

α	β	C_N	$C_{m_{c.g.}}$	c.p.	C_Y	C_n	C_l
2.0	0.0	0.0368	0.0041	50.1	0.0009	0.0002	0.0001
	1.0	.0372	.0044	50.0	-.0035	-.0016	.0001
	2.0	.0366	.0047	49.7	-.0078	-.0033	.0
	3.0	.0365	.0048	49.7	-.0130	-.0050	-.0001
	4.0	.0364	.0049	49.6	-.0180	-.0067	.0001
	5.0	.0375	.0051	49.6	-.0238	-.0080	.0001
	6.0	.0380	.0053	49.5	-.0308	-.0091	-.0002
	7.0	.0385	.0054	49.5	-.0389	-.0099	-.0003
↓	8.0	.0383	.0052	49.6	-.0473	-.0103	.0005
4.0	0.0	0.0812	0.0092	50.1	0.0019	0.0004	0.0010
	1.0	.0818	.0095	50.0	-.0028	-.0016	.0007
	2.0	.0825	.0100	49.9	-.0071	-.0032	.0007
	3.0	.0822	.0103	49.8	-.0123	-.0050	.0004
	4.0	.0824	.0107	49.7	-.0175	-.0065	.0003
	5.0	.0831	.0110	49.6	-.0237	-.0079	.0003
	6.0	.0837	.0110	49.7	-.0308	-.0090	.0002
	7.0	.0847	.0110	49.7	-.0394	-.0100	.0
↓	8.0	.0855	.0108	49.8	-.0472	-.0105	.0001
6.0	0.0	0.1262	0.0137	50.2	0.0021	0.0003	0.0008
	1.0	.1259	.0138	50.2	-.0027	-.0017	.0007
	2.0	.1259	.0141	50.1	-.0073	-.0035	.0006
	3.0	.1266	.0149	50.0	-.0132	-.0054	.0005
	4.0	.1266	.0153	49.9	-.0186	-.0068	.0005
	5.0	.1273	.0154	49.9	-.0248	-.0082	.0004
	6.0	.1289	.0156	49.9	-.0321	-.0094	.0003
↓	7.0	.1296	.0158	49.9	-.0407	-.0104	.0001
6.1	8.0	.1302	.0159	49.9	-.0486	-.0109	-.0002
8.0	0.0	0.1730	0.0165	50.5	0.0026	0.0003	.0007
	1.0	.1727	.0167	50.5	-.0027	-.0016	.0008
	2.0	.1727	.0170	50.4	-.0080	-.0035	.0005
	3.0	.1722	.0176	50.3	-.0138	-.0053	.0003
	4.0	.1728	.0184	50.2	-.0200	-.0068	.0
↓	5.0	.1735	.0191	50.2	-.0266	-.0082	-.0001
	5.9	.1746	.0200	50.1	-.0335	-.0096	-.0009
8.1	6.9	.1760	.0204	50.0	-.0420	-.0104	-.0008
8.1	7.9	.1775	.0208	50.0	-.0506	-.0110	-.0009

TABLE II.- STATIC LONGITUDINAL AND LATERAL AERODYNAMIC CHARACTERISTICS

OF AN AIRPLANE CONFIGURATION AND VARIOUS COMBINATIONS OF ITS

COMPONENTS. BODY AXIS DATA. M = 4.06.

R = 2.7 × 10^6 - Continued

(c) Body-wing - Concluded

α	β	c_N	$c_{m_{c.g.}}$	c.p.	c_Y	c_n	c_l
10.0	0.0	0.2275	0.0185	50.8	0.0038	0.0003	-0.0001
	1.0	.2278	.0189	50.8	-.0027	-.0015	-.0005
	2.0	.2279	.0195	50.7	-.0086	-.0032	-.0006
	3.0	.2279	.0200	50.7	-.0154	-.0051	-.0008
	3.9	.2274	.0213	50.5	-.0220	-.0065	-.0012
	4.9	.2234	.0225	50.4	-.0292	-.0077	-.0013
10.1	5.9	.2251	.0234	50.3	-.0366	-.0089	-.0014
10.1	6.9	.2267	.0243	50.2	-.0449	-.0100	-.0015
10.1	7.9	.2271	.0250	50.2	-.0538	-.0110	-.0017
12.0	0.0	0.2858	0.0196	51.1	0.0040	0.0004	-0.0004
	1.0	.2855	.0194	51.1	-.0030	-.0013	-.0009
	2.0	.2850	.0199	51.1	-.0097	-.0028	-.0011
	2.9	.2851	.0211	51.0	-.0176	-.0045	-.0013
	3.9	.2834	.0232	50.8	-.0244	-.0057	-.0023
	4.9	.2811	.0247	50.7	-.0324	-.0068	-.0027
12.1	5.9	.2819	.0262	50.5	-.0408	-.0079	-.0028
12.1	6.9	.2818	.0278	50.4	-.0494	-.0090	-.0032
12.1	7.8	.2824	.0292	50.3	-.0577	-.0100	-.0031

(d) Body-tail

α	β	c_N	$c_{m_{c.g.}}$	c.p.	c_Y	c_n	c_l
0.0	0.0	-0.0027	0.0002	54.4	-0.0006	0.0	0.0002
	1.0	-.0027	.0002	54.4	-.0119	.0025	.0001
	2.0	-.0033	.0	52.7	-.0232	.0050	.0006
	3.0	-.0038	.0003	54.5	-.0355	.0077	.0007
	4.0	-.0033	.0004	55.4	-.0469	.0102	.0008
	5.0	-.0027	.0004	56.1	-.0586	.0128	.0005
2.0	0.0	0.0202	-0.0113	65.5	0.0001	-0.0001	0.0004
	1.0	.0202	-.0113	65.5	-.0114	.0026	.0003
	2.0	.0202	-.0116	65.8	-.0225	.0051	.0002
	3.0	.0202	-.0118	66.0	-.0348	.0078	.0
	4.0	.0202	-.0119	66.2	-.0470	.0104	.0001
	5.0	.0206	-.0122	66.2	-.0586	.0128	.0005

TABLE II.- STATIC LONGITUDINAL AND LATERAL AERODYNAMIC CHARACTERISTICS

OF AN AIRPLANE CONFIGURATION AND VARIOUS COMBINATIONS OF ITS

COMPONENTS. BODY AXIS DATA. M = 4.06.

$R = 2.7 \times 10^6$ - Concluded

(d) Body-tail - Concluded

α	β	C_N	$C_{m_{c.g.}}$	c.p.	C_Y	C_n	C_l
4.0	0.0	0.0417	−0.0253	66.6	0.0008	−0.0001	−0.0003
	0.0	.0433	−.0246	65.7	.0013	−.0002	.0001
	1.0	.0422	−.0254	66.4	−.0114	.0025	.0002
	1.0	.0431	−.0246	65.7	−.0109	.0025	−.0001
	2.0	.0422	−.0255	66.5	−.0224	.0050	.0007
	2.0	.0431	−.0249	65.9	−.0221	.0050	−.0002
	3.0	.0427	−.0257	66.4	−.0347	.0077	.0006
	3.0	.0441	−.0254	65.9	−.0346	.0077	−.0001
	4.0	.0433	−.0260	66.4	−.0476	.0104	.0004
	4.0	.0445	−.0259	66.0	−.0474	.0104	.0005
	5.0	.0445	−.0264	66.2	−.0600	.0129	.0001
↓	5.0	.0445	−.0264	66.2	−.0599	.0129	.0007
6.0	0.0	0.0686	−0.0394	65.8	0.0015	−0.0002	0.0004
	1.0	.0691	−.0395	65.8	−.0110	.0026	.0003
	2.0	.0691	−.0397	65.8	−.0224	.0050	−.0001
	3.0	.0691	−.0393	65.7	−.0361	.0079	−.0003
↓	4.0	.0690	−.0396	65.8	−.0480	.0105	−.0003
8.0	0.0	0.0951	−0.0552	66.0	0.0016	−0.0002	0.0009
	1.0	.0953	−.0552	65.9	−.0113	.0025	.0007
↓	2.0	.0953	−.0547	65.8	−.0228	.0049	.0006

TABLE III.- STATIC LONGITUDINAL AERODYNAMIC CHARACTERISTICS OF AN

AIRPLANE CONFIGURATION AND VARIOUS COMBINATIONS OF ITS

COMPONENTS. STABILITY AXIS DATA.

$M = 4.06.$ $R = 2.7 \times 10^6.$

(a) Body-wing-tail

α	β	C_L	C_{D_T}	C_{D_B}	L/D_T	α	β	C_L	C_{D_T}	C_{D_B}	L/D_T
0.0	0.0	-0.0023	0.0439	0.0056	-0.05	6.0	0.0	0.1555	0.0646	0.0056	2.41
2.0	0.0	.0468	.0475	.0056	.99	8.0	0.0	.2053	.0780	.0055	2.63
4.0	0.0	.0975	.0534	.0056	1.83						
4.0	0.0	.0977	.0528	.0056	1.85						

(b) Body

α	β	C_L	C_{D_T}	C_{D_B}	L/D_T	α	β	C_L	C_{D_T}	C_{D_B}	L/D_T
0.0	0.0	-0.0017	0.0156	0.0053	-0.11	12.0	0.0	0.0847	0.0382	0.0058	2.22
2.0	0.0	.0061	.0165	.0053	.37	14.0	0.0	.1038	.0463	.0058	2.24
4.0	0.0	.0166	.0181	.0053	.92	15.0	0.0	.1127	.0509	.0058	2.21
6.0	0.0	.0307	.0209	.0053	1.47	16.0	0.0	.1219	.0558	.0058	2.18
8.0	0.0	.0471	.0256	.0058	1.84	18.0	0.0	.1446	.0680	.0058	2.13
10.0	0.0	.0665	.0312	.0058	2.13	20.0	0.0	.1676	.0829	.0058	2.02

(c) Body-wing

α	β	C_L	C_{D_T}	C_{D_B}	L/D_T	α	β	C_L	C_{D_T}	C_{D_B}	L/D_T
0.0	0.0	0.0045	0.0293	0.0052	0.15	8.0	0.0	0.1667	0.0567	0.0055	2.94
2.0	0.0	.0357	.0314	.0052	1.14	10.0	0.0	.2180	.0738	.0058	2.95
4.0	0.0	.0788	.0364	.0052	2.16	12.0	0.0	.2721	.0946	.0057	2.88
6.0	0.0	.1222	.0449	.0052	2.72						

(d) Body-tail

α	β	C_L	C_{D_T}	C_{D_B}	L/D_T	α	β	C_L	C_{D_T}	C_{D_B}	L/D_T
0.0	0.0	-0.0027	0.0329	0.0056	-0.08	6.0	0.0	0.0646	0.0414	0.0056	1.56
2.0	0.0	.0190	.0343	.0056	.55	8.0	0.0	.0892	.0484	.0055	1.84
4.0	0.0	.0408	.0367	.0056	1.11						
4.0	0.0	.0393	.0364	.0056	1.08						
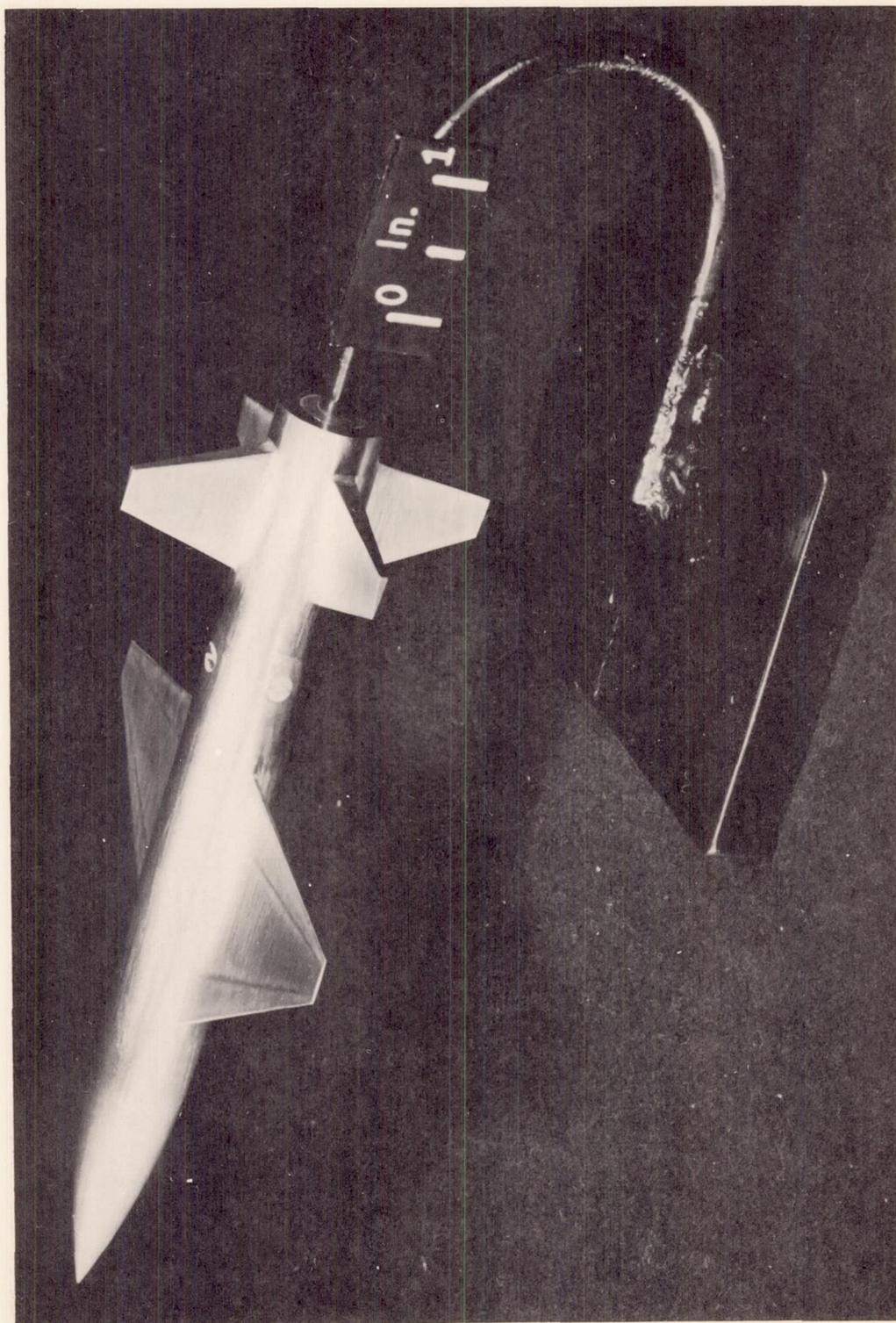
L-86688

Figure 1.- Photograph of complete-model configuration.
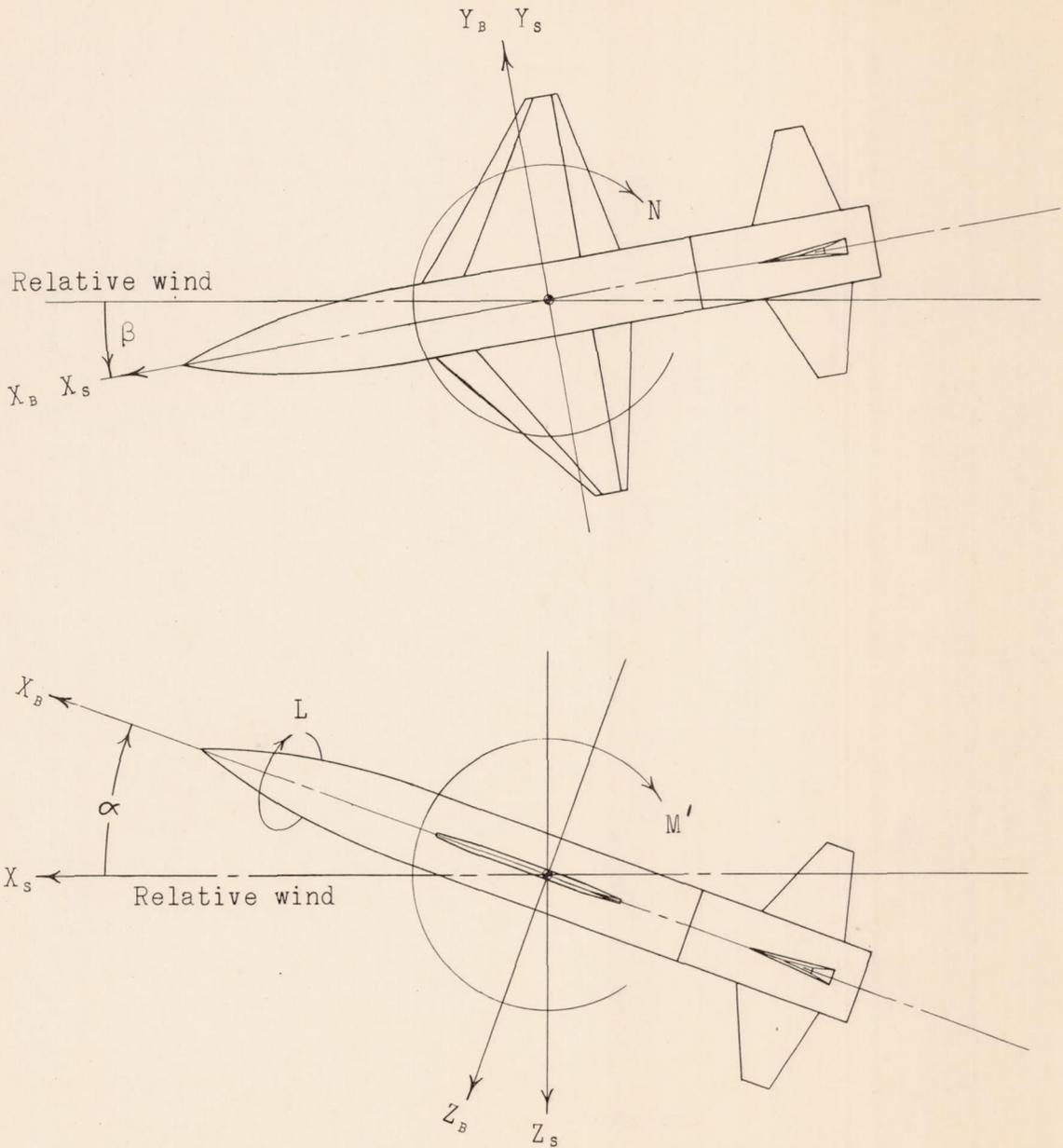
Figure 2.- Systems of reference axes. Subscript B indicates body
axes; subscript S indicates stability axes.
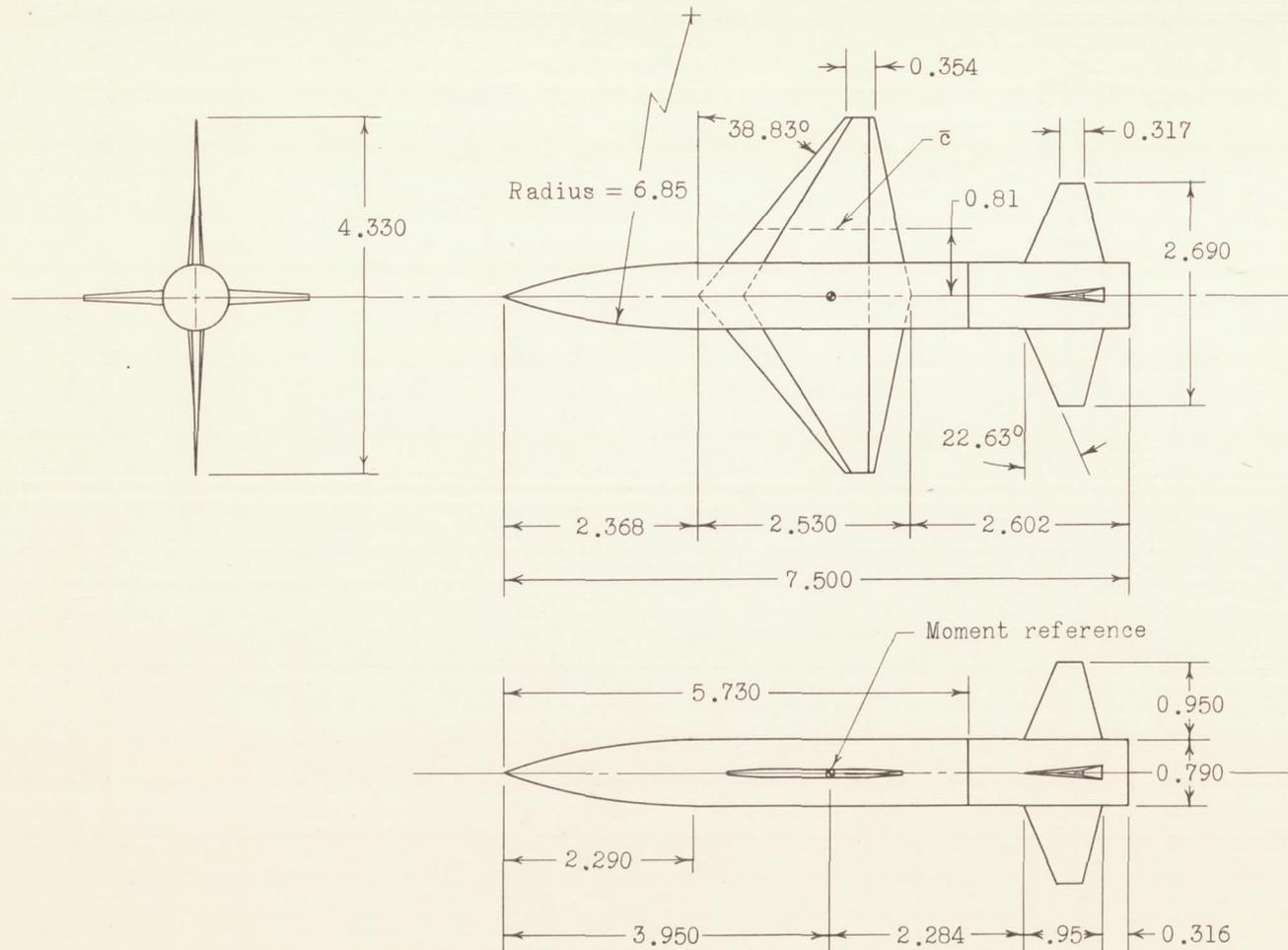
Figure 3(a).- Wind-tunnel model. All dimensions are in inches.

.01 c radius   .04 c   .02 c

.20 c

.80 c

c

(a) Wing.

.007 in. radius

10°

c_t
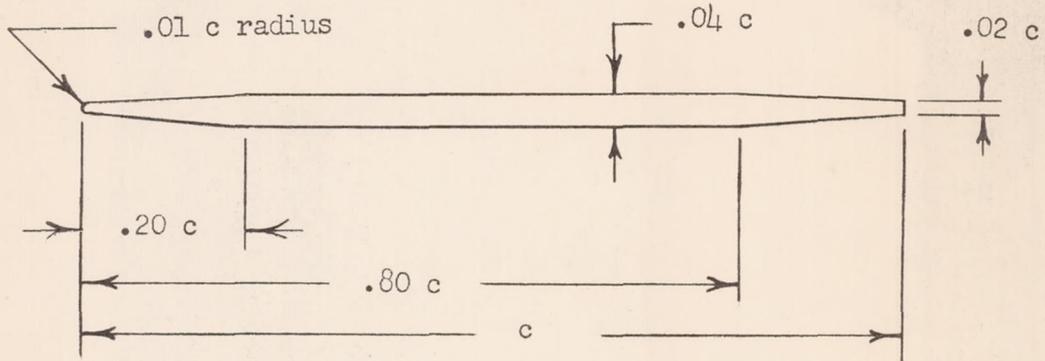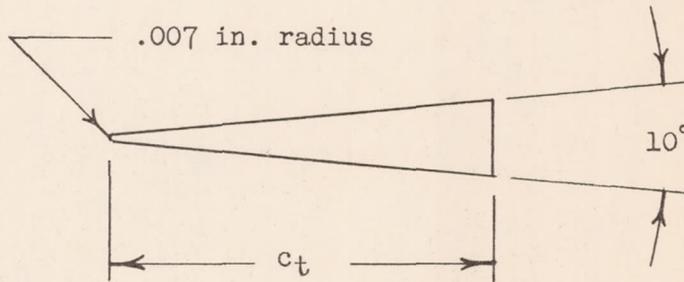
(b) Horizontal and vertical tails.

Figure 3(b).- Wing and tail airfoil sections used on model.
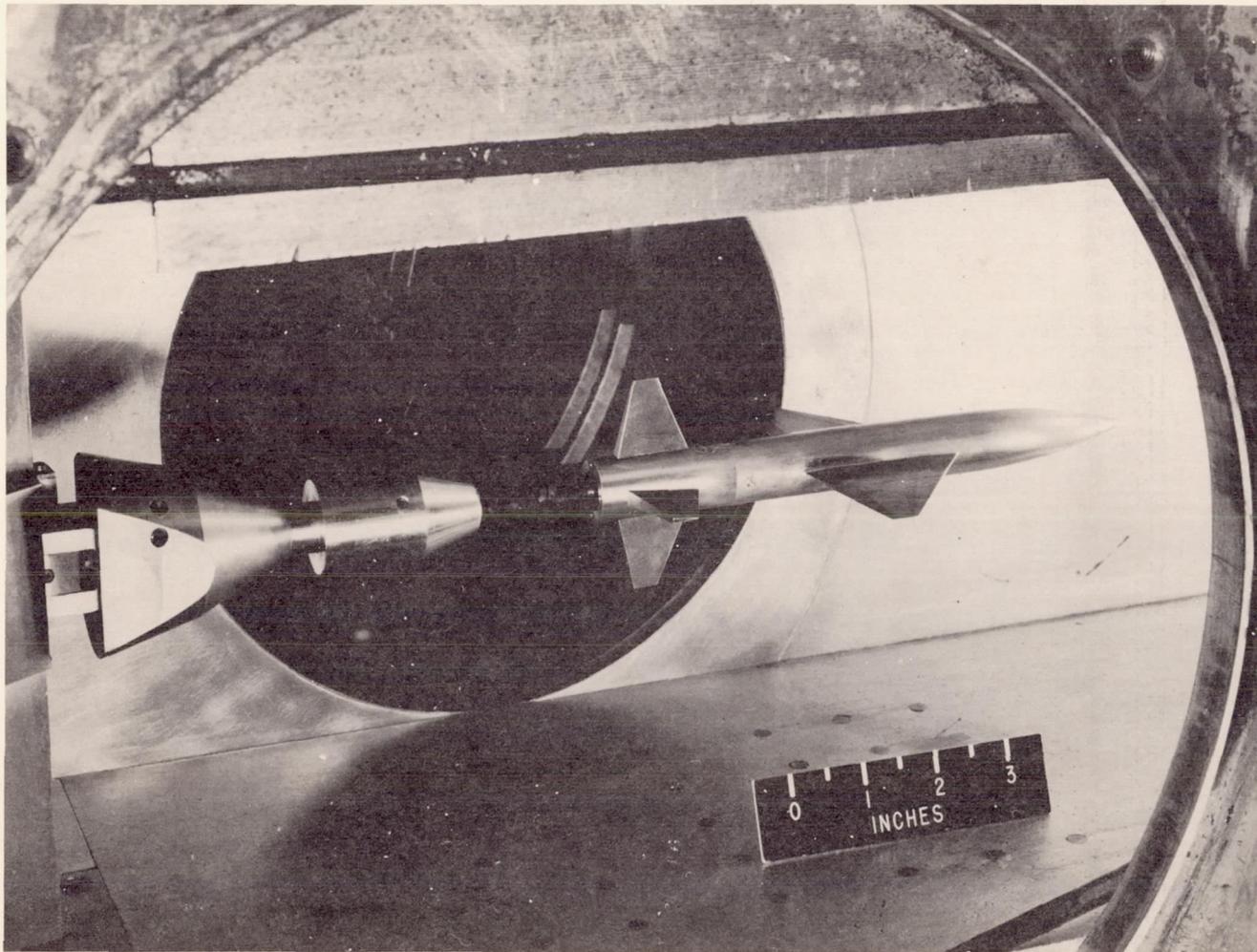
L-87425

Figure 4.- Installation of the wind-tunnel model in the Langley 9- by
9-inch Mach number 4 blowdown jet.
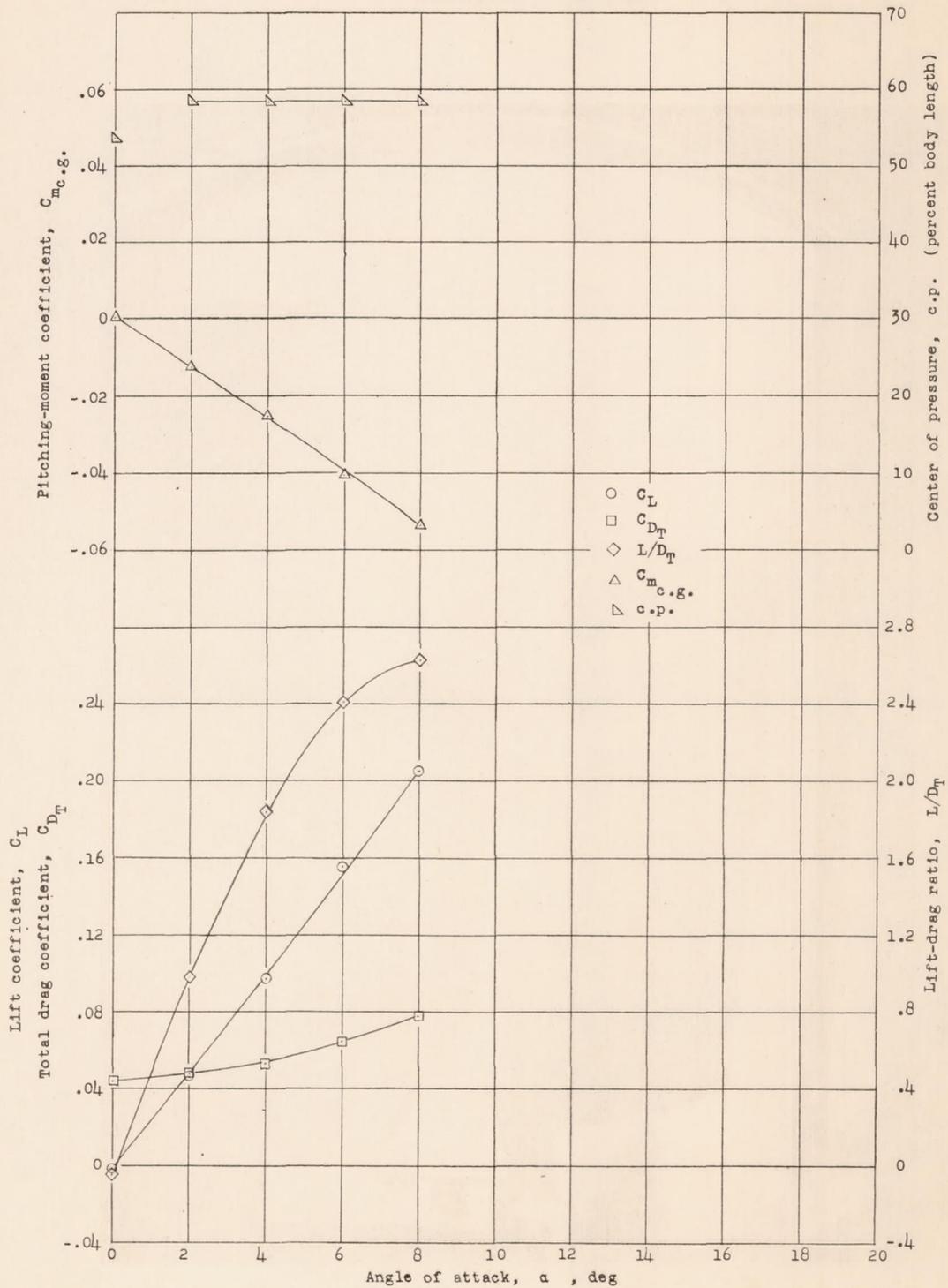
(a) Body-wing-tail.

Figure 5.- Variation with angle of attack of the static longitudinal characteristics of an airplane configuration and its components. $M = 4.06$; $R = 2.7 \times 10^6$.
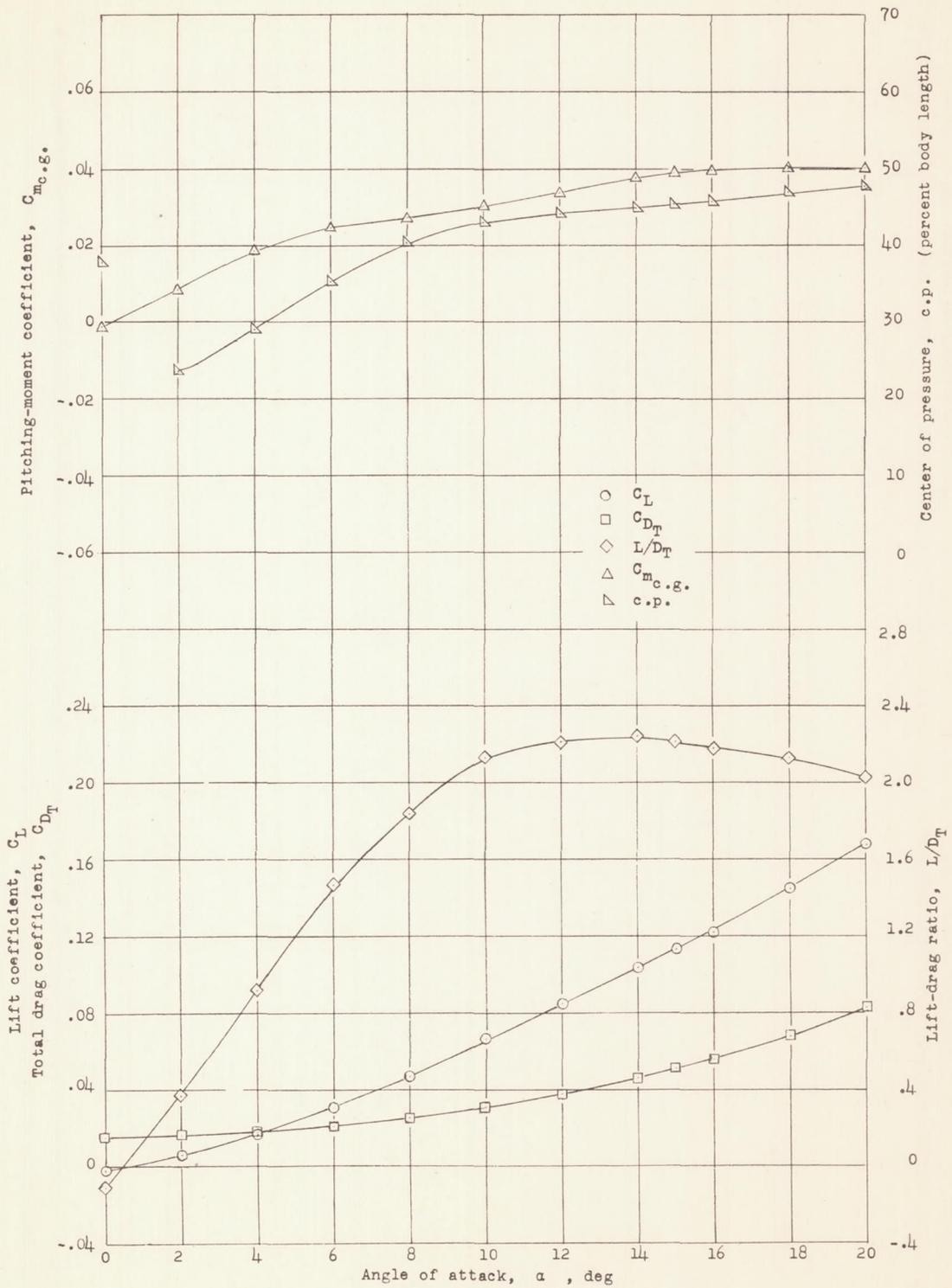
(b) Body.

Figure 5.- Continued.
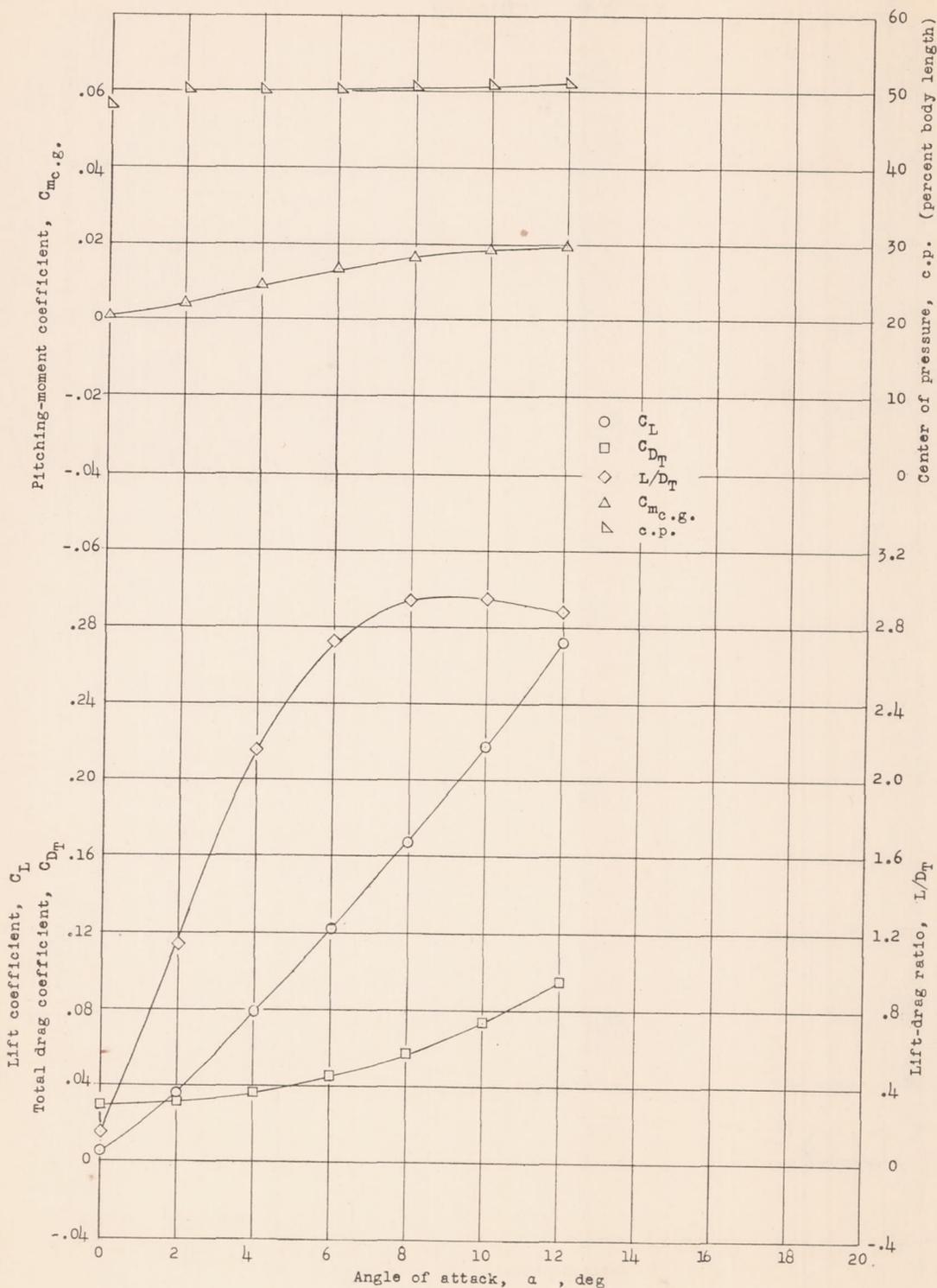
(c) Body-wing.

Figure 5.- Continued.
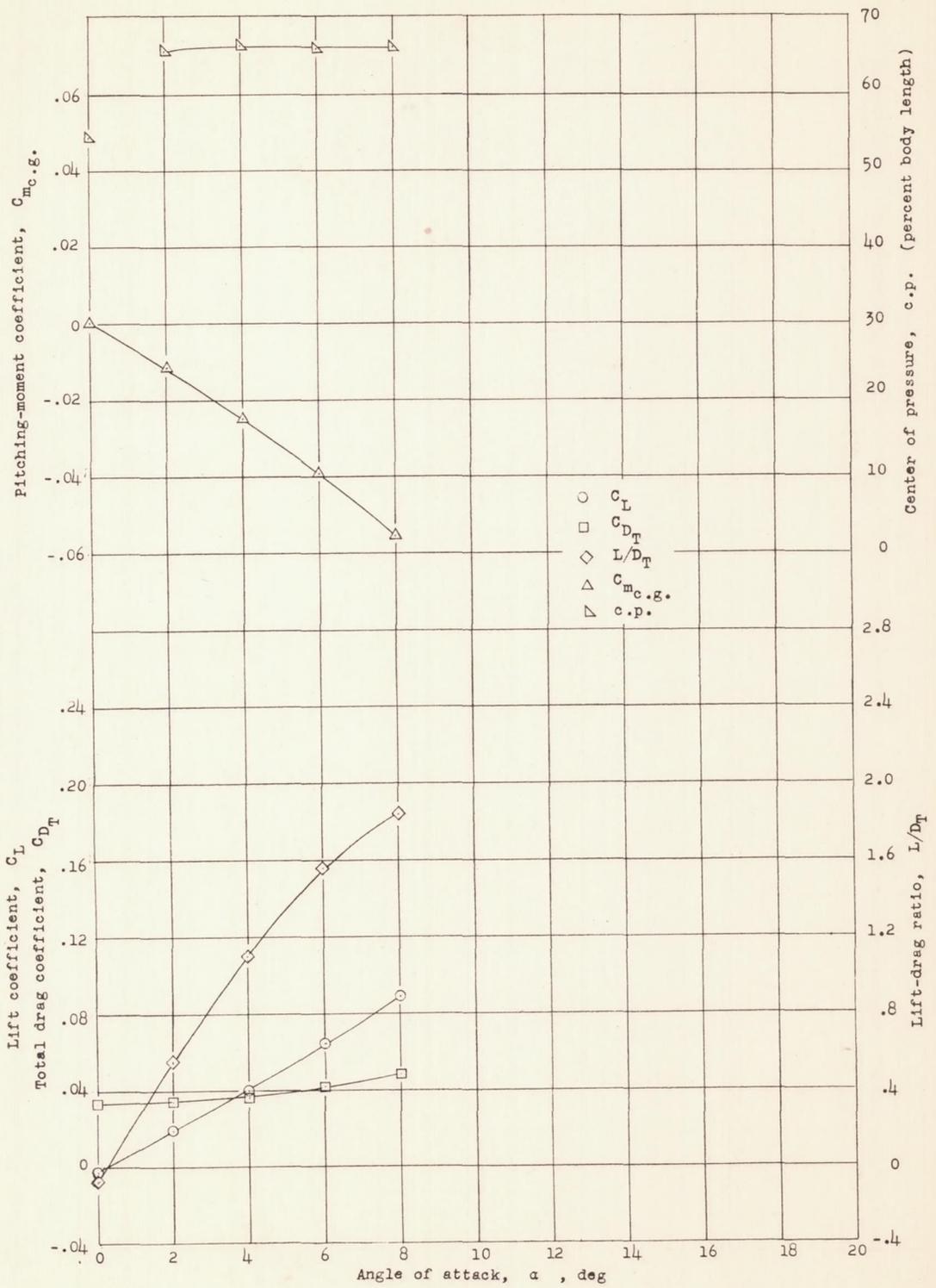
(d) Body-tail.

Figure 5.- Concluded.
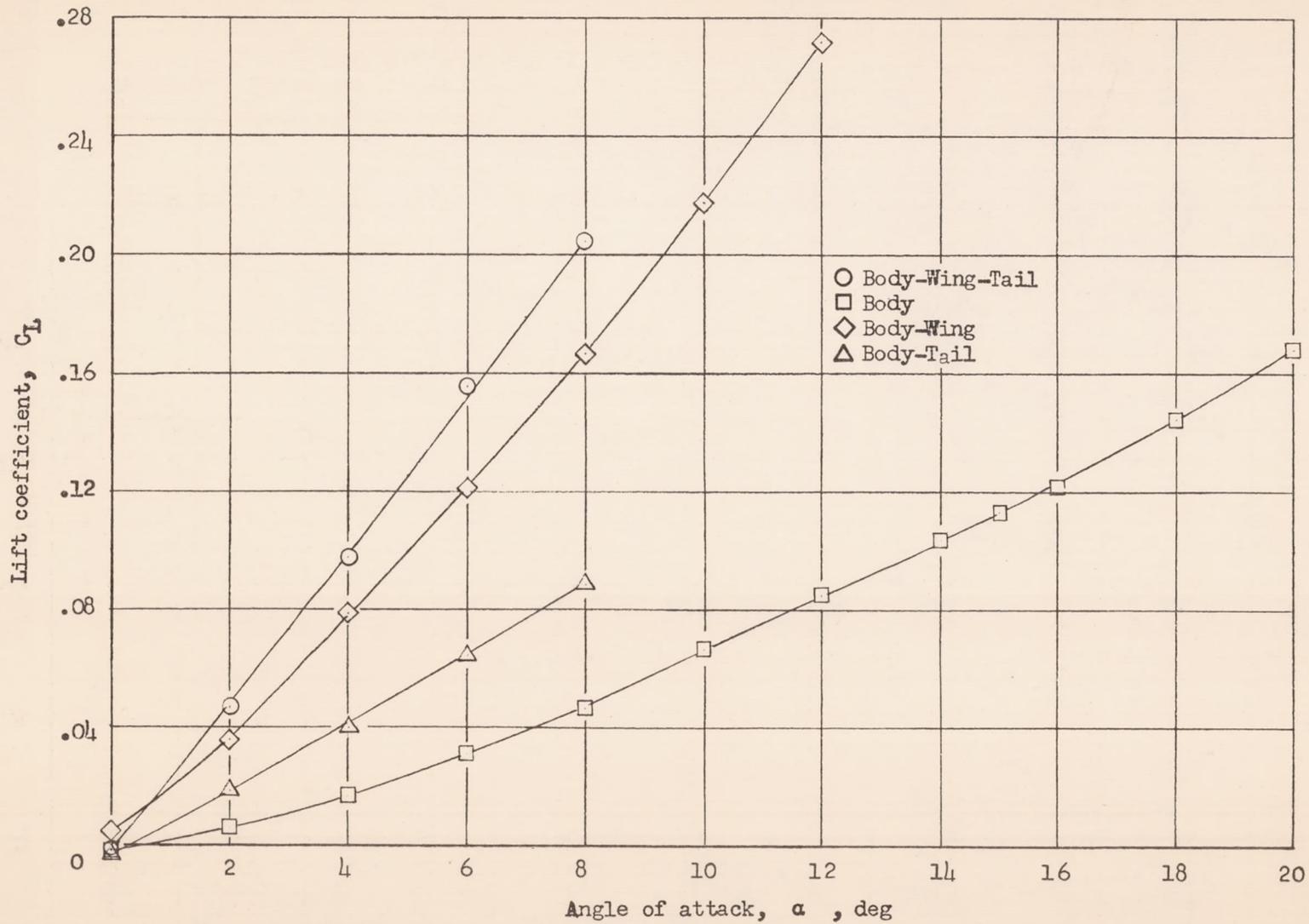
Figure 6.- Variation of lift coefficient with angle of attack for an airplane configuration and its components. M = 4.06; R = 2.7 × 10^6.
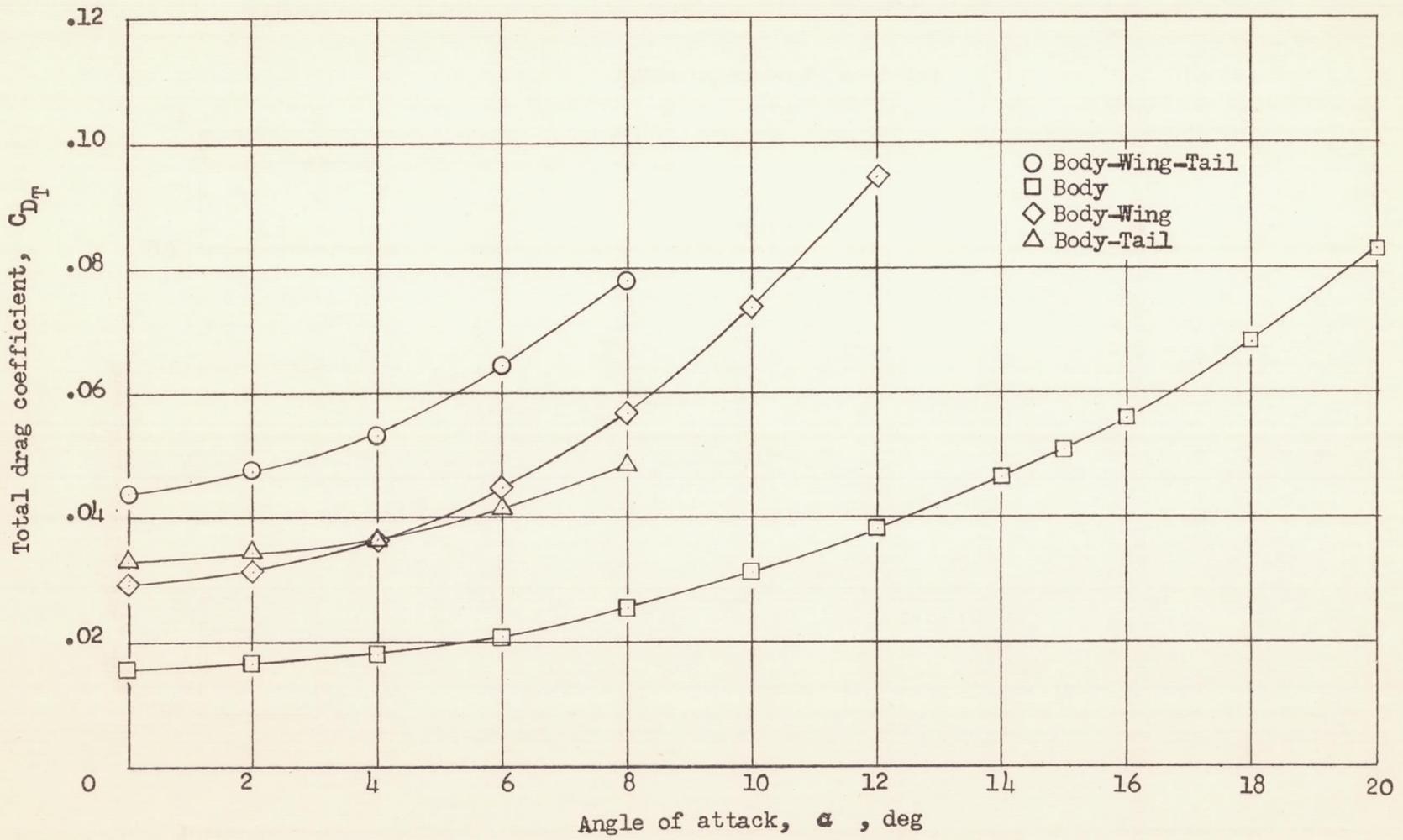
Figure 7.- Variation of total drag coefficient with angle of attack for
an airplane configuration and its components. M = 4.06; R = 2.7 × 10⁶.
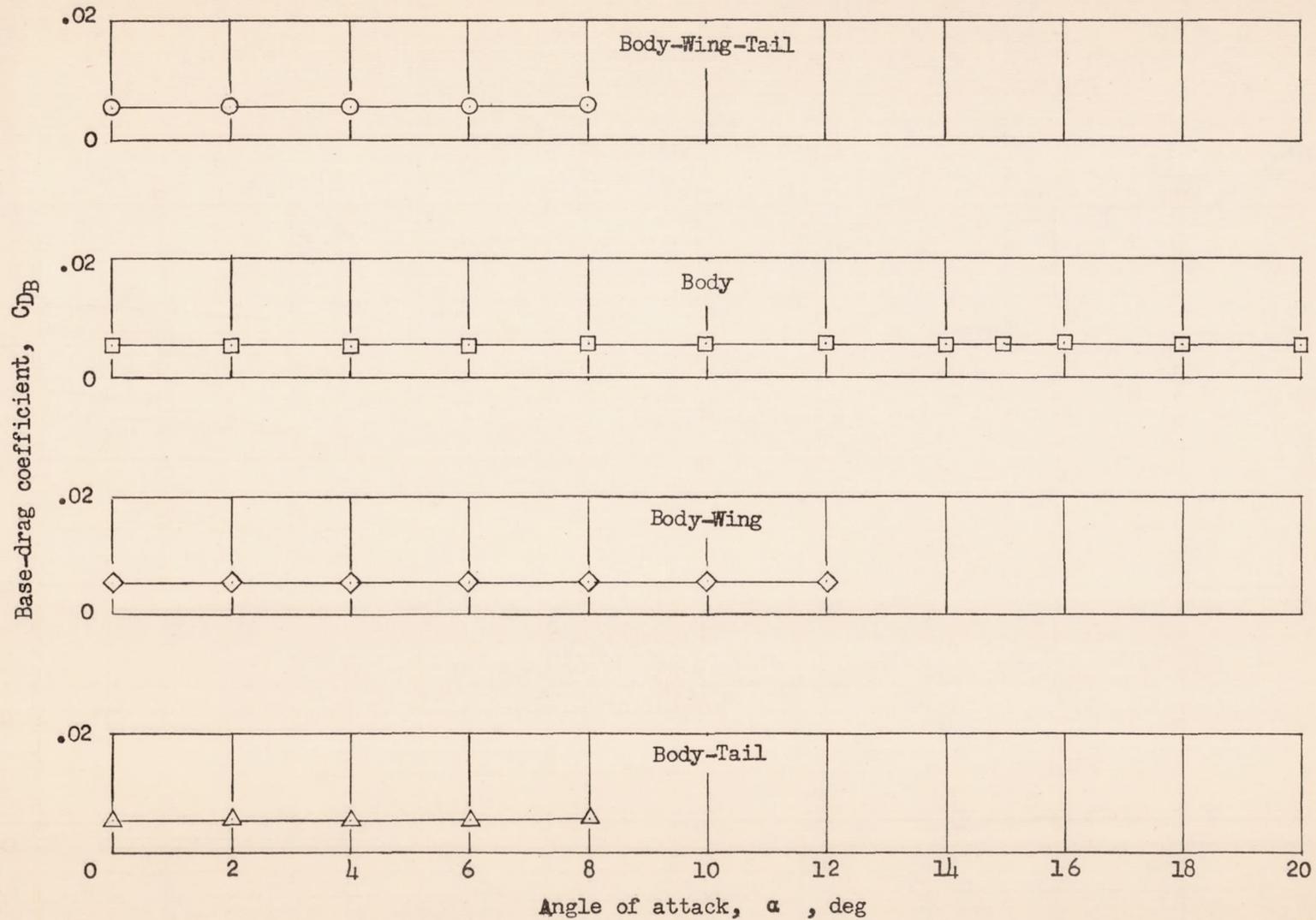
Figure 8.- Variation of base drag coefficient with angle of attack for an airplane configuration and its components. $M = 4.06$; $R = 2.7 \times 10^6$.
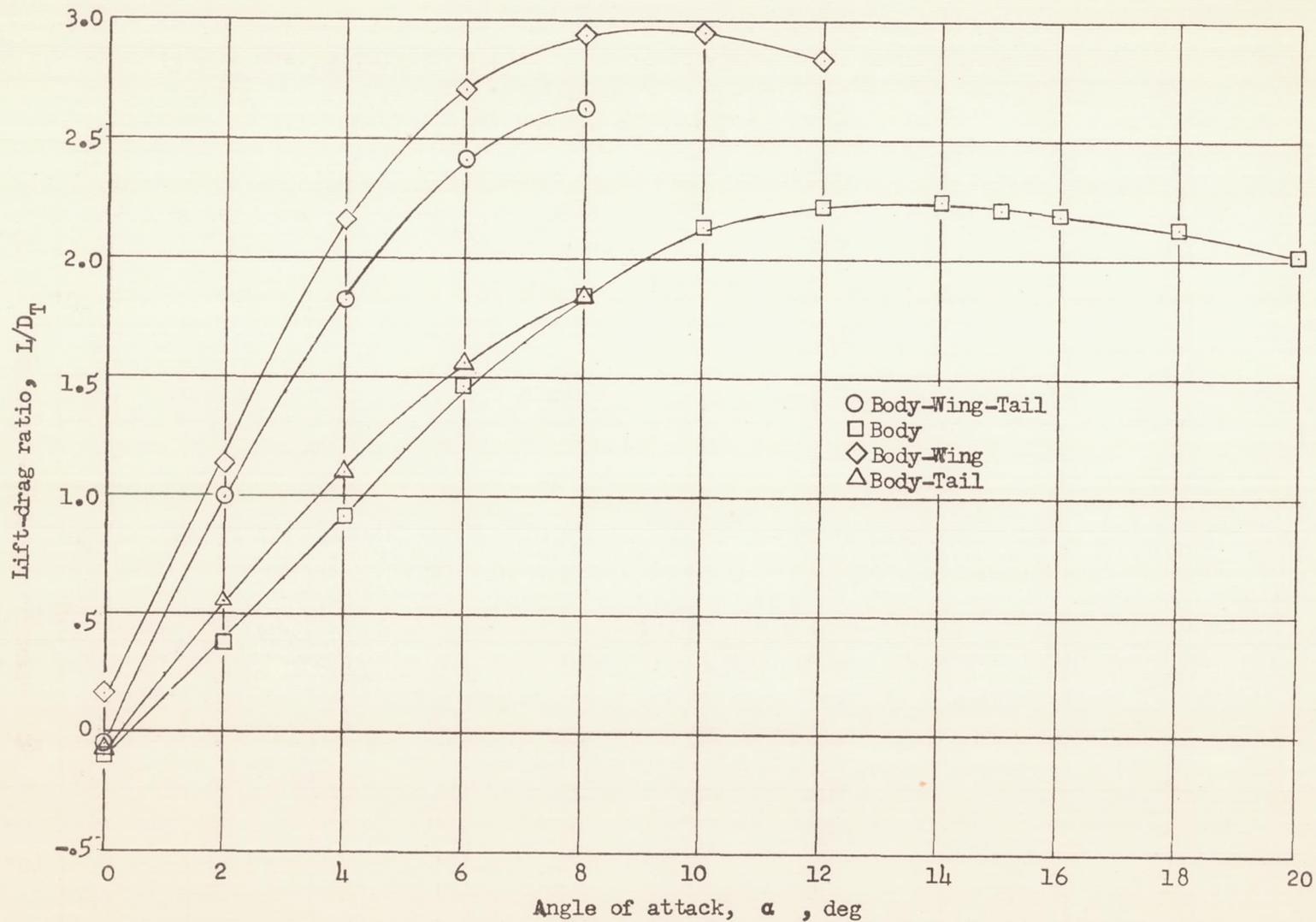
Figure 9.- Variation of lift-drag ratio with angle of attack for an airplane configuration and its components. $M = 4.06$; $R = 2.7 \times 10^6$.
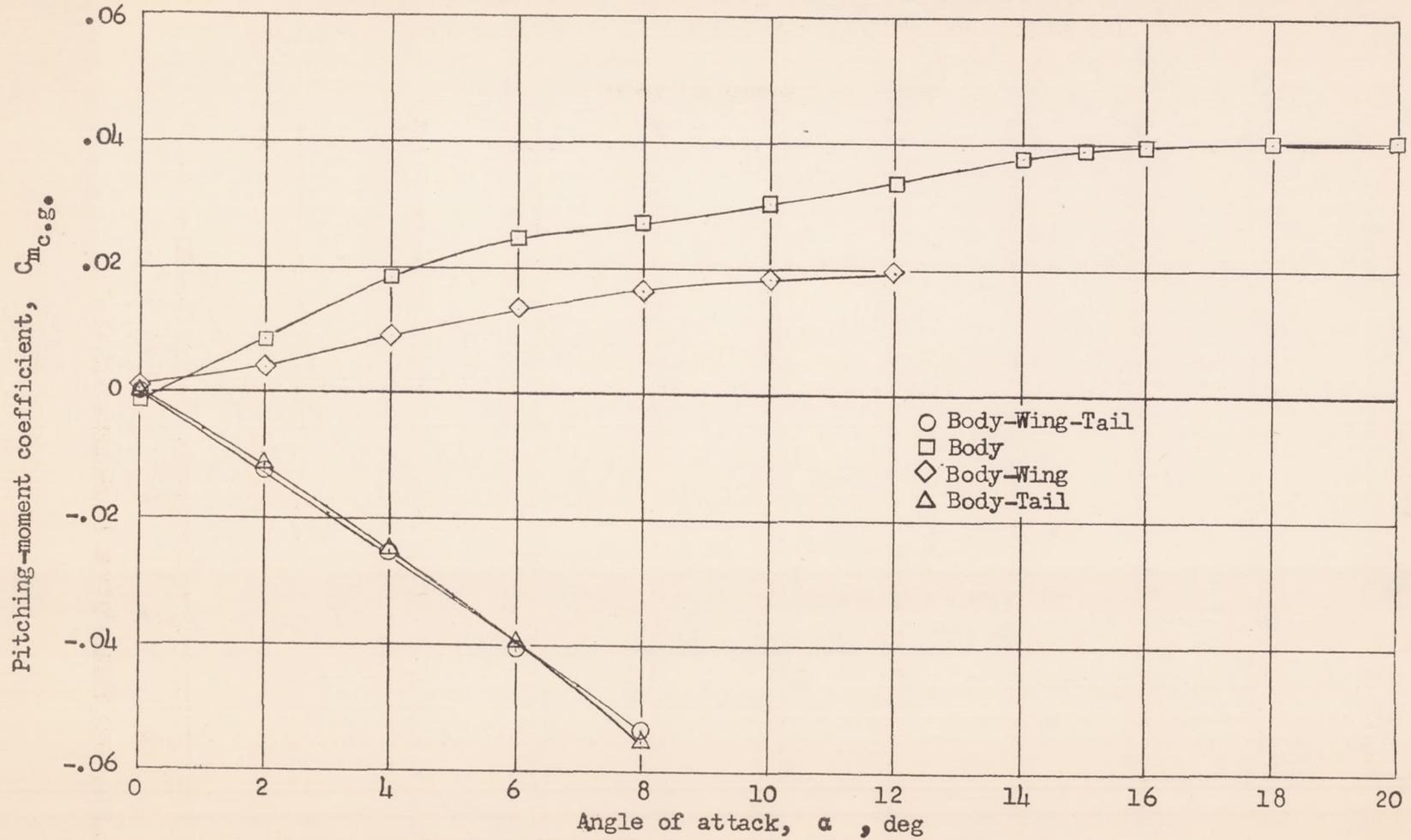
Figure 10.- Variation of pitching-moment coefficient with angle of attack for an airplane configuration and its components. M = 4.06; R = 2.7 × 10^6.
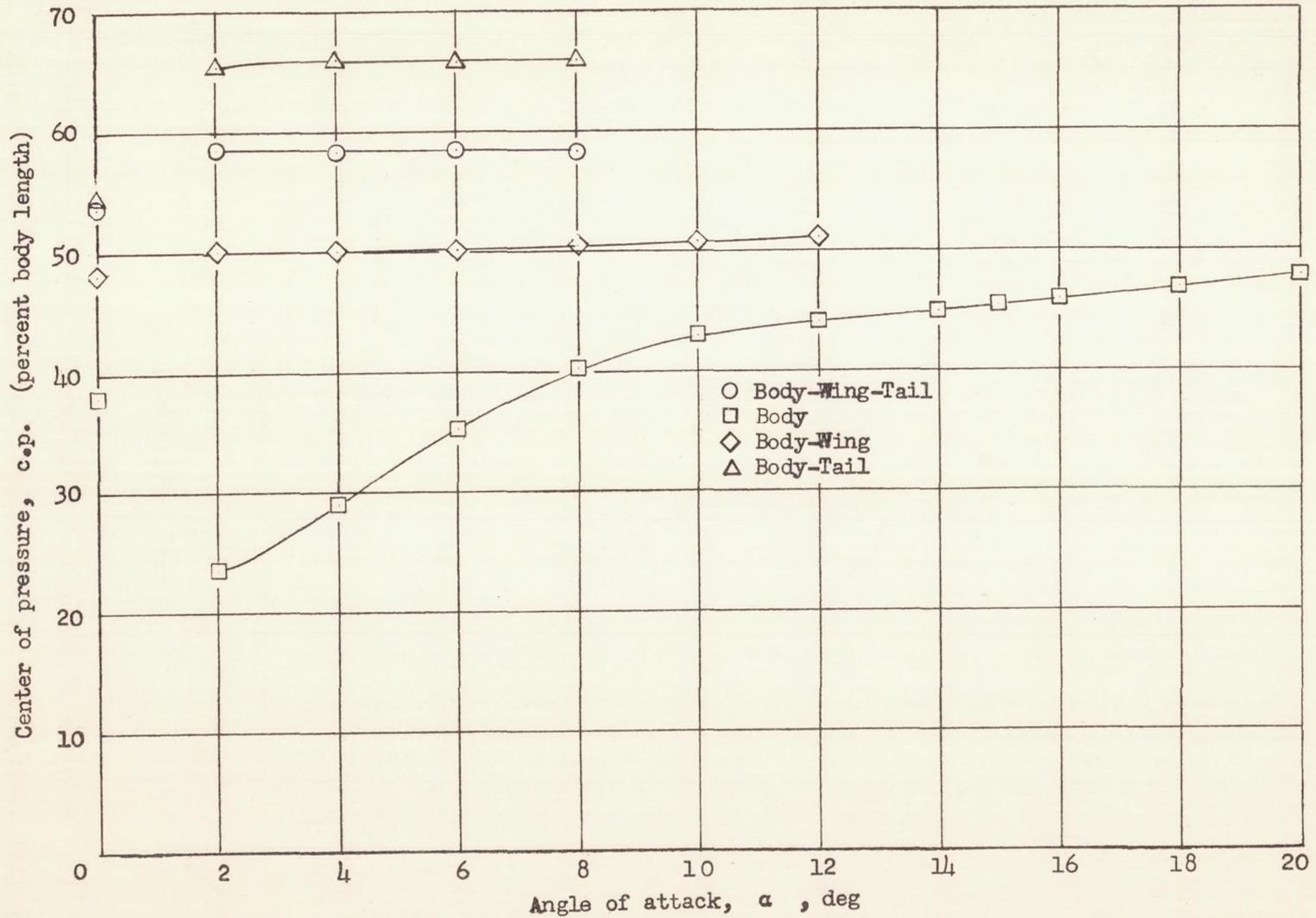
Figure 11.- Variation of longitudinal center of pressure with angle of attack for an airplane configuration and its components. M = 4.06.
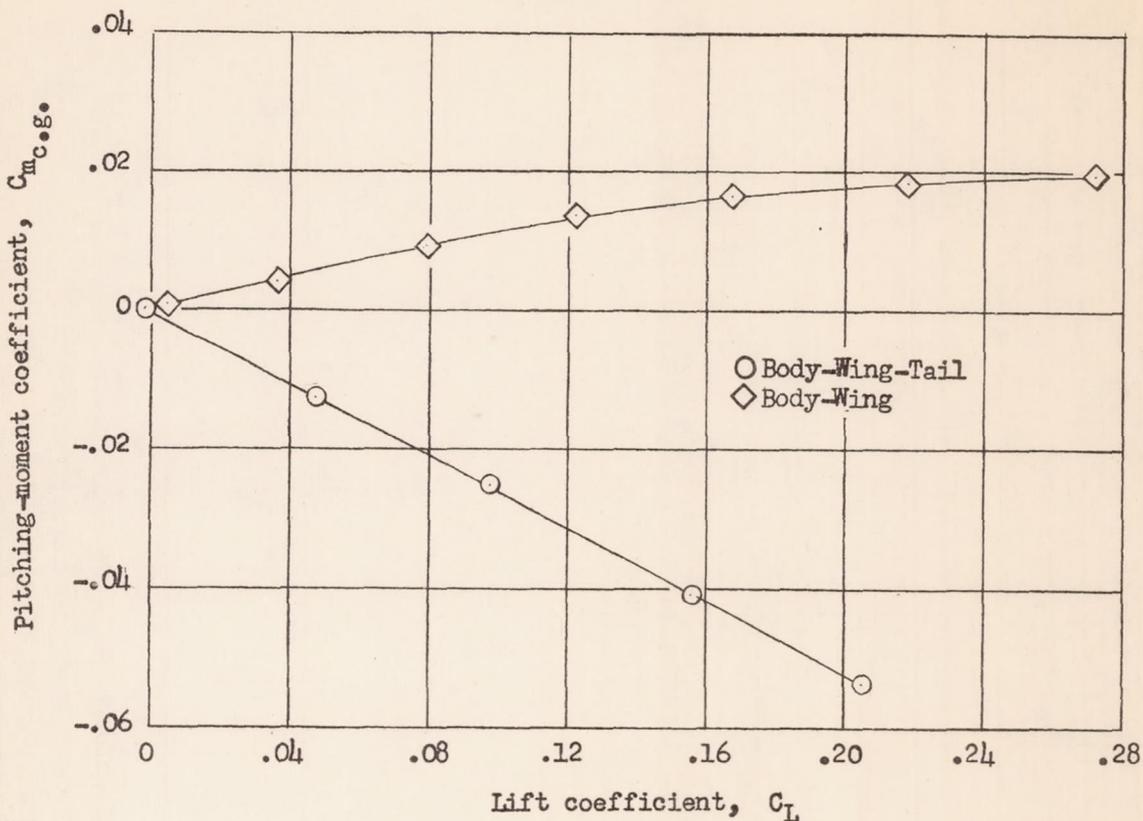
Figure 12.- Variation of pitching-moment coefficient with lift coefficient for an airplane configuration with and without tail fins. M = 4.06.
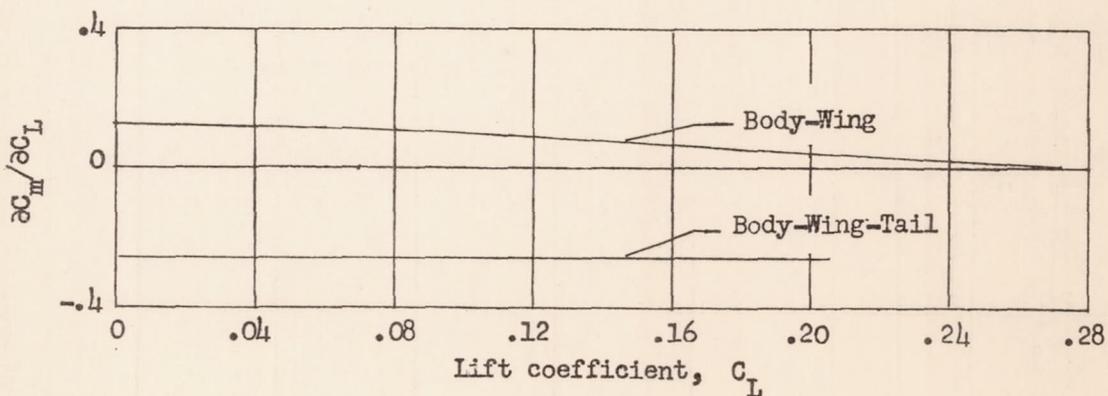
Figure 13.- Variation of the static-longitudinal-stability parameter $\frac{\partial C_m}{\partial C_L}$ with lift coefficient for the complete model and for the body-wing configuration. M = 4.06.
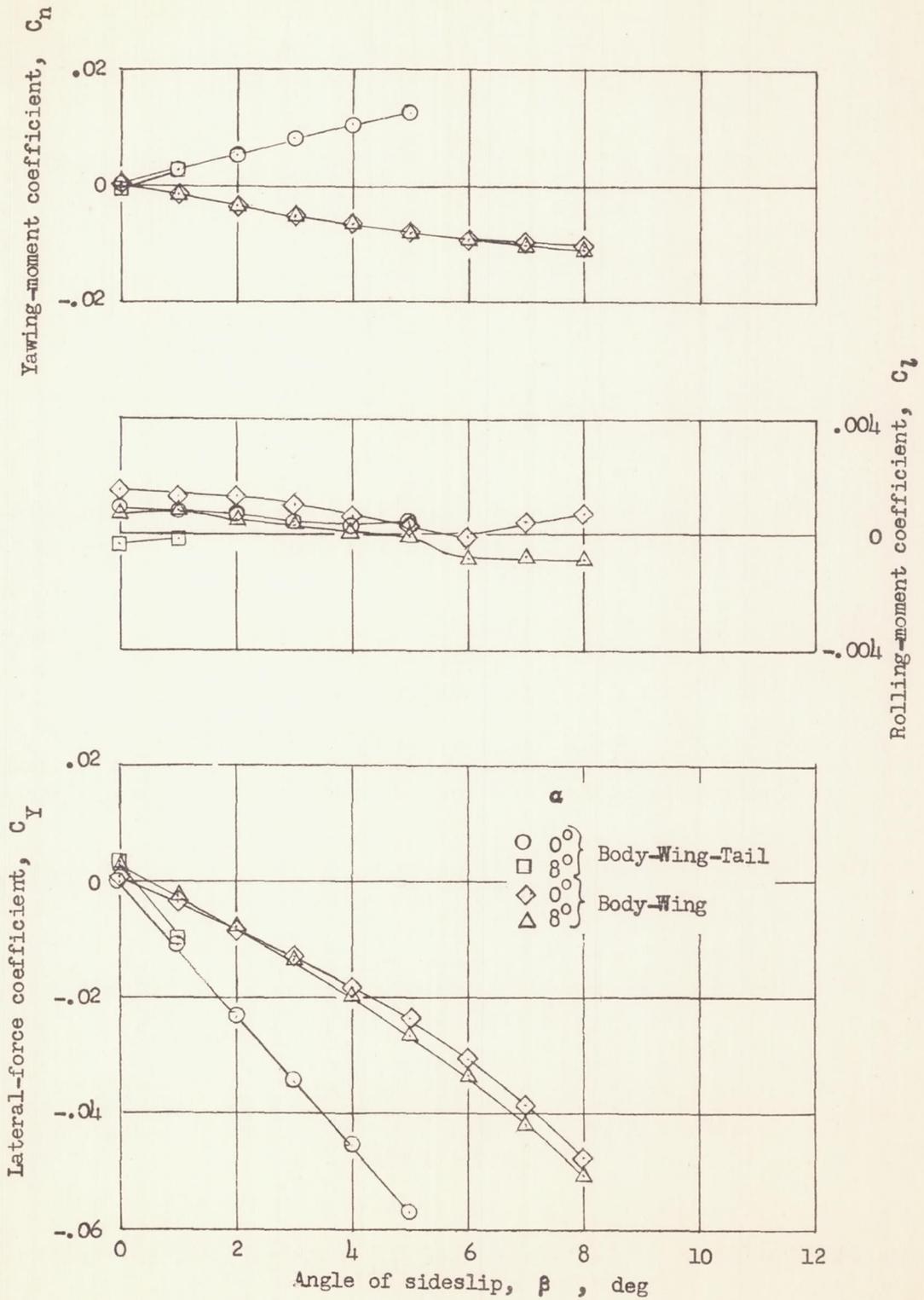
Figure 14.- Variation with angle of sideslip of the static lateral
    characteristics for an airplane configuration with and without
    tail fins. M = 4.06; R = 2.7 × 10^6.
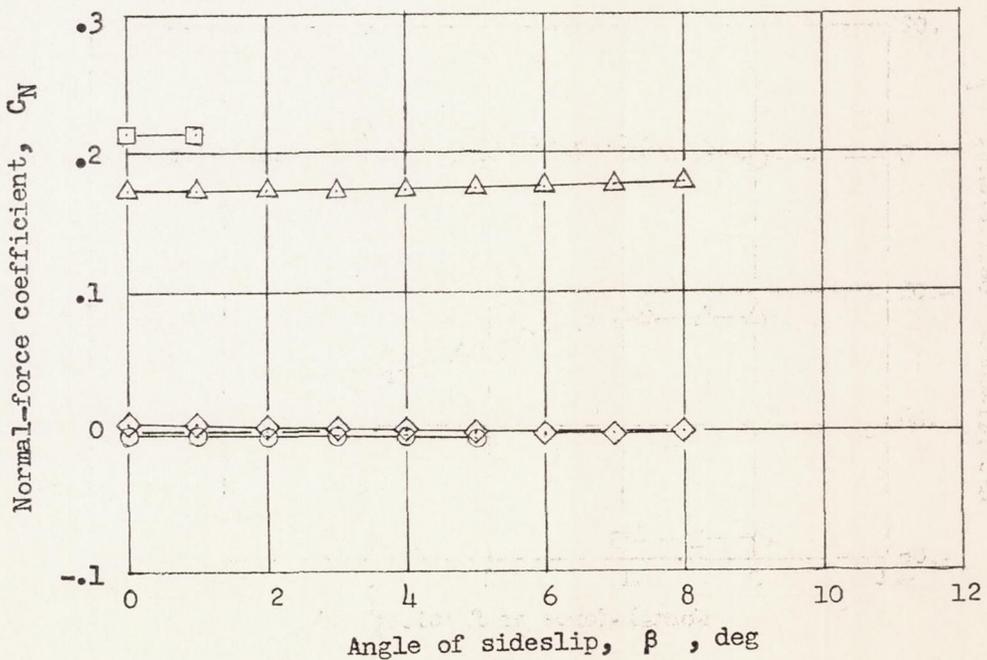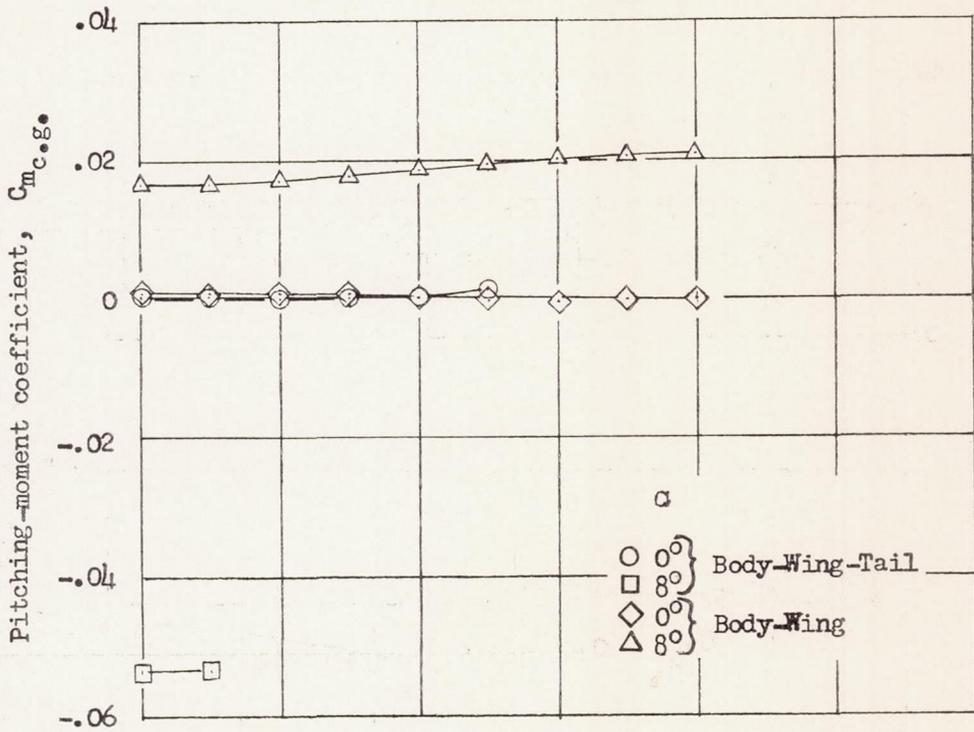
Figure 15.- Variation with angle of sideslip of the static longitudinal
   characteristics for an airplane configuration with and without tail
   fins. M = 4.06; R = 2.7 × 10^6.
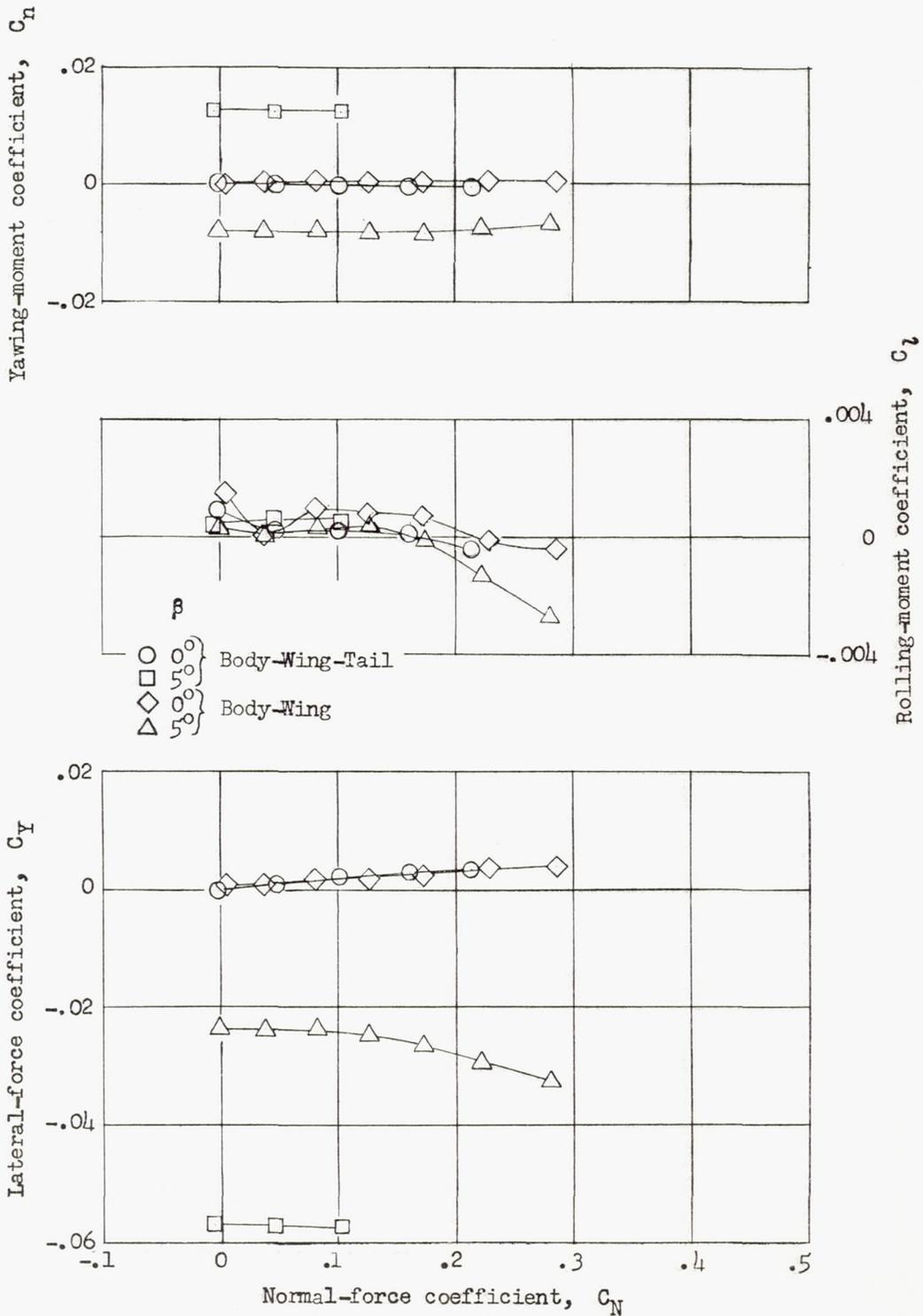
Figure 16.- Variation with normal-force coefficient of the static lateral
characteristics for an airplane configuration with and without tail
fins. M = 4.06; R = 2.7 × 10⁶.
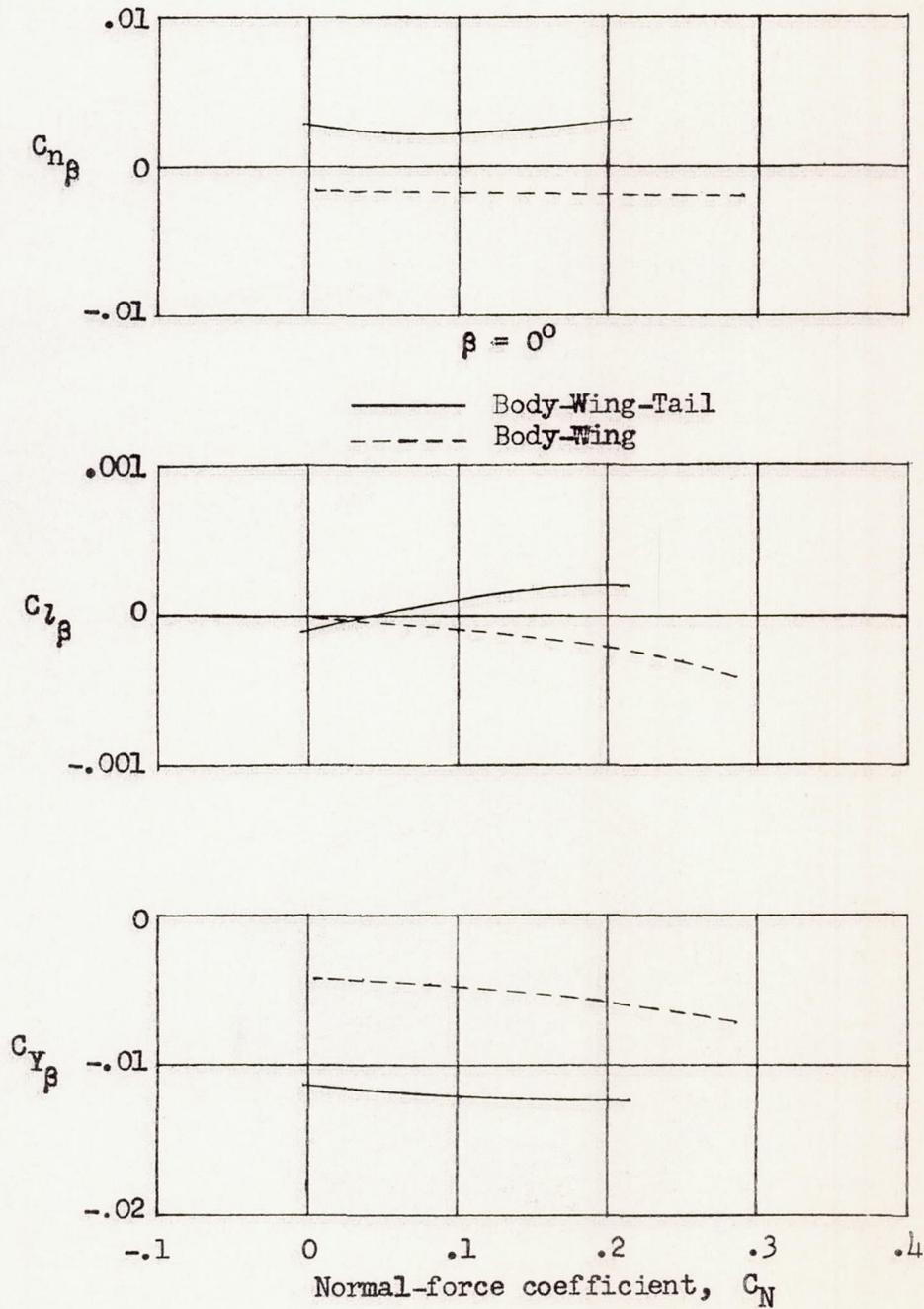
Figure 17.- Variation with normal-force coefficient of the rate of change of the static lateral force coefficients with β for an airplane configuration with and without tail fins. M = 4.06; R = 2.7 × 10^6.
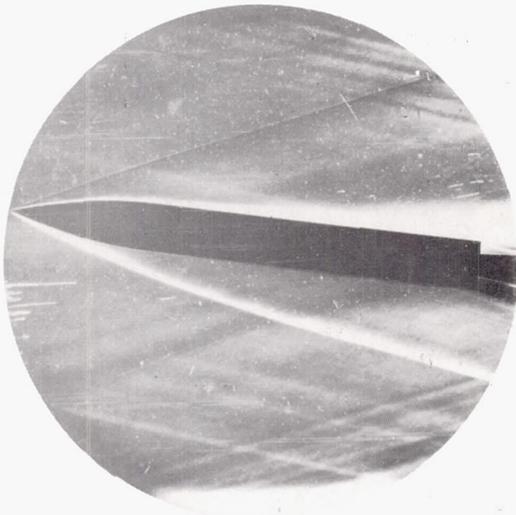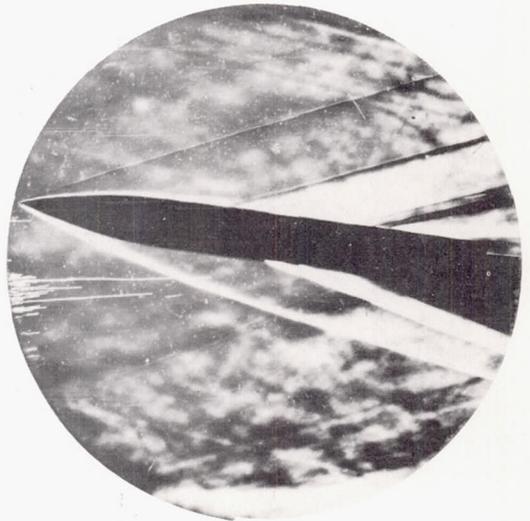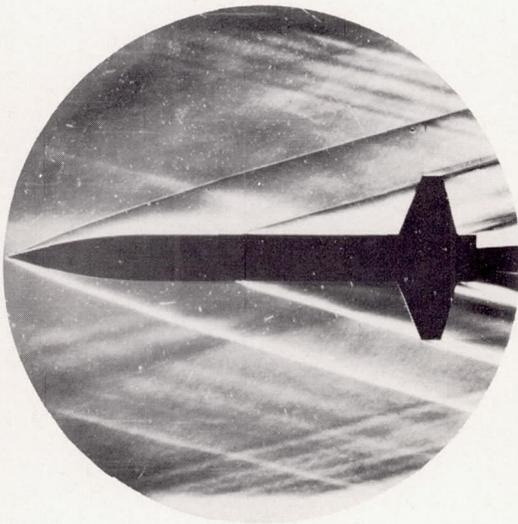
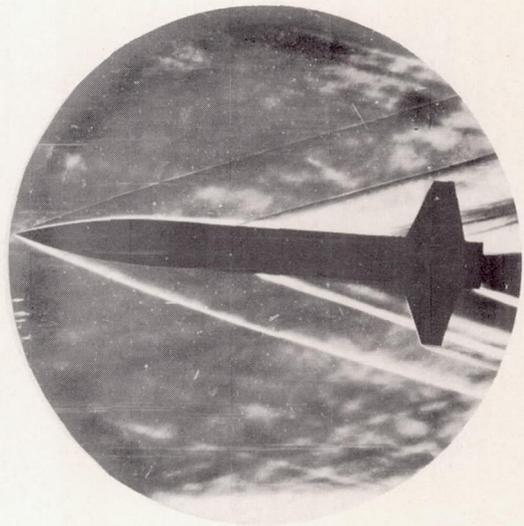Body alone   Body-wing
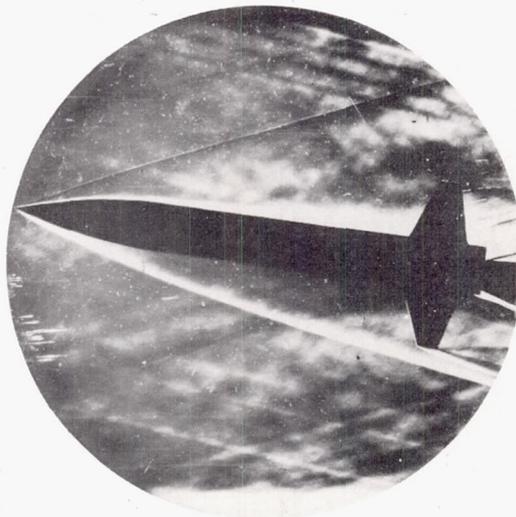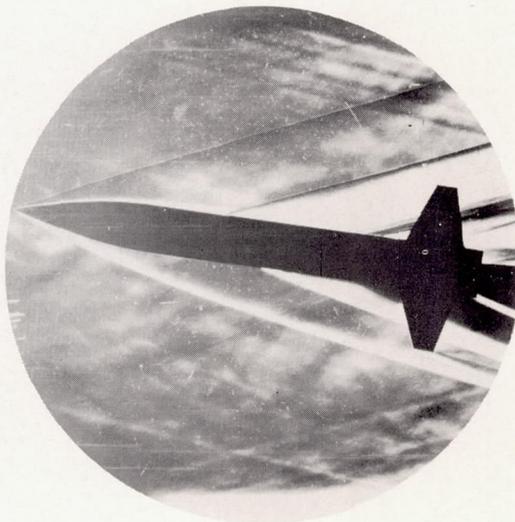
Body-tail

L-87529

Figure 18.- Schlieren photographs of the flow around the body-alone,
body-wing, and body-tail configurations. $\alpha = 8^\circ$; $\beta = 0^\circ$; $M = 4.06$.

$\alpha = 0^o$

$\alpha = 4^o$

$\alpha = 8^o$

L-87530

Figure 19.- Schlieren photographs of the flow around the complete-airplane configuration.　$\beta = 0^o$; $M = 4.06$.